

Contact and Solvent-Separated Geminate Radical Ion Pairs in Electron-Transfer Photochemistry

Ian R. Gould,*[†] Ralph H. Young,*[‡] Roger E. Moody,^{†,§} and Samir Farid*[†]

Corporate Research Laboratories, Eastman Kodak Company, Rochester, New York 14650-2109, and Research and Technology Development, Copy Products Division, Eastman Kodak Company, Rochester, New York 14650-2021 (Received: June 22, 1990; In Final Form: December 5, 1990)

The two primary intermediates that play a major role in determining the efficiencies of bimolecular photoinduced electron-transfer reactions are the contact ($A^{\cdot-}D^{+\cdot}$) and the solvent-separated ($A^{\cdot-}(S)D^{+\cdot}$) radical ion pairs, CRIP and SSRIP, respectively. These two species are distinguished by differences in electronic coupling, which is much smaller for the SSRIP compared to the CRIP, and solvation, which is much larger for the SSRIP compared to the CRIP. The present work addresses the quantitative aspects of these and other factors that influence the rates of energy-wasting return electron transfer within the ion-pair intermediates. The electron acceptor tetracyanoanthracene (TCA) forms ground-state charge-transfer complexes with alkyl-substituted benzene donors. By a change of the excitation wavelength and/or donor concentration, either the free TCA or the CT complex can be excited. Quenching of free $^1TCA^*$ by the alkylbenzene donors that have low oxidation potentials, such as pentamethylbenzene and hexamethylbenzene, in acetonitrile solution leads to the direct formation of geminate SSRIP. Excitation of the corresponding charge-transfer complexes leads to the formation of geminate CRIP. Rates of return electron transfer within the two types of ion pair are determined from quantum yields for formation of free radical ions together with the CRIP fluorescence decay lifetimes. The rates of return electron transfer within both sets of radical ion pairs depend upon the reaction exothermicity in a manner consistent with the Marcus inverted region. The data are analyzed by using a golden rule model in which the rate is given as a function of an electronic coupling matrix element, reorganization energies for the rearranged high-frequency (skeletal vibration) and low-frequency (mainly solvent and libration) motions, and an averaged frequency for the skeletal modes. Estimates for the reorganization energies and the skeletal frequency for the CRIP are obtained independently by analysis of the spectral distribution of the CRIP (exciplex) emission spectrum. A good fit to the return electron-transfer rate data for the CRIP is obtained by using the values for these parameters obtained from the emission spectrum. It is found that the electronic coupling in the CRIP is ca. 2 orders of magnitude higher than in the SSRIP and that the intermolecular (mainly solvent) reorganization energy for the contact pair is ca. 1 eV lower than that of the solvent-separated pair. The relevance of these observations to the photophysical and photochemical properties of contact radical ion pairs is discussed.

Introduction

Bimolecular photoinduced electron transfer from a donor to an acceptor in homogeneous solution results in the efficient formation of geminate radical ion pairs.^{1,2} As demonstrated by the pioneering work of Weller et al., two types of radical ion pair are usually implicated in polar solvents, namely, the contact radical ion pair (CRIP) and the solvent-separated radical ion pair (SSRIP).¹ These descriptions have historical precedence in the organic chemistry of solvolysis reactions.³ Solvent-separated and contact ion pairs are distinguished in such reactions by the "special salt" effect.³ In photochemical reactions the two types of radical ion pair can be further distinguished by the higher electronic coupling in the contact pair, which results in a measurable probability of emission from these species, and the possibility of mixing of other (locally) excited states with the pure ion state.^{1,2} The weak electronic coupling in the solvent-separated radical ion pair results in a very small singlet/triplet energy gap, so that intersystem crossing between the two spin states can be modulated by the application of weak magnetic fields.^{1,4} The solvent-separated radical ion pairs are also expected to be more highly solvated than the contact pairs.

Bimolecular photoinduced electron-transfer reactions are usually carried out in polar solvents to enable solvation and separation processes to produce free radical ions in solution. Many chemical reactions of the resulting radical ions have been reported,⁵ and in some cases different products have been identified from the free-radical ions and the geminate radical ion pairs.⁶ In polar solvents such as acetonitrile, the importance of the SSRIP has been emphasized.^{1,2,6} In less polar solvents the CRIP are more important since solvation to form the SSRIP becomes endothermic and less likely to occur.^{1,2} The CRIP can be considered to be a

special case of the well-known exciplex.^{1,2} The term exciplex is used to describe species that are characterized by a wide range of mixing between ionic and locally excited states, i.e., varying degrees of charge-transfer (CT) character. When an ionic state is considerably lower in energy than the locally excited states, then very little mixing with these other states will occur and the exciplex is equivalent to a pure CRIP. A CRIP can be produced upon photochemical excitation of a ground-state charge-transfer (CT) complex.⁷ As with exciplexes, excited CT complexes are essentially pure CRIP, if mixing with other electronic states is negligible. The photochemistry and photophysics of excited CT complexes,^{8,9} and especially of exciplexes^{1,2,5,10} have been the

(1) (a) Beens, H.; Weller, A. In *Organic Molecular Photophysics*; Birks, J. B., Ed.; Wiley: London, 1975; Vol. 2, Chapter 4. (b) Weller, A. *Z. Phys. Chem. (Wiesbaden)* **1982**, *130*, 129. (c) Weller, A. *Z. Phys. Chem. (Wiesbaden)* **1982**, *133*, 93.

(2) (a) Masuhara, H.; Mataga, N. *Acc. Chem. Res.* **1981**, *14*, 312. (b) Mataga, N. *Pure Appl. Chem.* **1984**, *56*, 1255. (c) Mataga, N.; Okada, T.; Kanda, Y.; Shioyama, H. *Tetrahedron* **1986**, *42*, 6143.

(3) (a) Winstein, S.; Clippinger, E.; Fainberg, A. H.; Robinson, G. C. *J. Am. Chem. Soc.* **1954**, *76*, 2597. (b) Winstein, S.; Robinson, G. C. *J. Am. Chem. Soc.* **1958**, *80*, 169. (c) Fainberg, A. H.; Winstein, S. *J. Am. Chem. Soc.* **1956**, *78*, 2767. (d) Fainberg, A. H.; Robinson, G. C.; Winstein, S. *J. Am. Chem. Soc.* **1956**, *78*, 2777.

(4) (a) Schulten, K.; Staerk, H.; Weller, A.; Werner, H.-J.; Nickel, B. *Z. Phys. Chem. (Wiesbaden)* **1976**, *101*, 371. (b) Werner, H.-J.; Staerk, H.; Weller, A. *J. Chem. Phys.* **1978**, *68*, 2419. (c) Weller, A.; Staerk, H.; Treichel, R. *Faraday Discuss. Chem. Soc.* **1984**, *78*, 271.

(5) (a) Mattes, S. L.; Farid, S. In *Organic Photochemistry*; Padwa, A., Ed.; Marcel Dekker: New York, 1983; Vol. 6, p 233. (b) Davidson, R. S. In *Advances in Physical Organic Chemistry*; Gold, V., Bethell, D., Eds.; Academic Press: London, 1983; Vol. 19, p 1. (c) Mattes, S. L.; Farid, S. *Science* **1984**, *226*, 917. (d) Kavaros, G. J.; Turro, N. J. *Chem. Rev.* **1986**, *86*, 401. (e) *Photoinduced Electron Transfer. Part C. Photoinduced Electron Transfer Reactions: Organic Substrates*; Fox, M. A., Chanon, M., Eds.; Elsevier: Amsterdam, 1988. (f) Mattay, J. *Synthesis* **1989**, 233.

(6) (a) Mattes, S. L.; Farid, S. *J. Chem. Soc., Chem. Commun.* **1980**, 126. (b) Mattes, S. L.; Farid, S. *J. Am. Chem. Soc.* **1983**, *105*, 1386. (c) Mattes, S. L.; Farid, S. *J. Am. Chem. Soc.* **1986**, *108*, 7356.

(7) Mulliken, R. S.; Pearson, W. B. *Molecular Complexes: A Lecture and Reprint Volume*; Wiley: New York, 1969.

* Corporate Research Laboratories.

[†] Research and Technology Development, Copy Products Division.

[‡] Current address: Analytical Technology Division, Eastman Kodak Company, Rochester, NY 14650-2132.

subject of many studies over the past 25 years. In several cases the differences in the behavior of contact and solvent-separated radical ion pairs have been investigated. For example, it has often been observed that irradiation of ground-state CT complexes results in virtually no formation of free radical ions even in a polar solvent,¹¹⁻¹³ whereas under similar conditions, free radical ion formation is often observed for bimolecular quenching of an excited donor or acceptor.^{1,2,5} In contrast to the many reported examples of exciplex emission,^{1,2,5} there are only a few reports of emission from the excited states of ground-state CT complexes.⁹ These observations suggest that nonradiative decay is very efficient in the CRIP that are formed by excitation of ground state CT complexes.

For photochemically produced radical ion pairs, the nonradiative deactivation process is a return electron-transfer reaction that regenerates the neutral starting materials. The rates of this process have been studied in detail for several SSRIP systems in acetonitrile^{12,14,15} and are found to be consistent with the theories of electron-transfer reactions. In particular a Marcus "inverted" region¹⁶ is observed, in which the rates decrease with increasing reaction exothermicity. Electron-transfer rates are sensitive to the extent of solvation of the donor and acceptor and to the extent of electronic coupling in these species. On the basis of the previous discussion it is thus expected that the rates of return electron transfer within the solvent-separated and contact radical ion pairs should be quite different. Specifically, when the Franck-Condon factors are favorable, the higher electronic coupling in the contact radical ion pairs should result in much higher electron-transfer rates compared to the solvent-separated radical ion pairs. Furthermore, the Franck-Condon factors themselves should be significantly different for the two sets of radical ion pairs, since in polar solvents these are dominated by solvation terms. The relative rates of return electron transfer in solvent-separated and contact radical ion pairs have been investigated previously.¹² For the systems that were investigated, it was demonstrated that the radical ion pairs formed by diffusive fluorescence quenching in acetonitrile were solvent-separated radical ion pairs (called loose ion pairs in ref 12b) and different from the contact radical ion pairs (compact ion pairs in ref 12b) formed by the excitation of ground-state CT complexes. It was also observed that the return electron-transfer

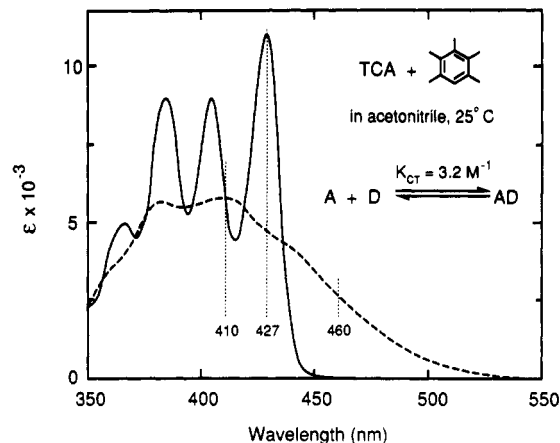


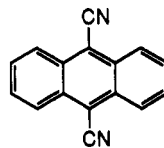
Figure 1. Absorption spectrum of TCA in acetonitrile at room temperature, together with the spectrum of the TCA/PMB charge-transfer complex obtained by extrapolation to infinite PMB concentration (see text).

rate constants were different for the two types of radical ion pair and that the rates had different dependencies on the reaction exothermicity. However, in those studies, donor-acceptor systems of different structural characteristics were compared, and, perhaps as a consequence, the differences in the rates for the two types of ion pair could not be explained by using current theories for electron-transfer reactions (vide infra).^{12b} In this work we describe a study in which the rates of return electron transfer within contact and solvent-separated radical ion pairs of the *same molecular species* in the same solvent, acetonitrile, are compared directly. In these systems the differences in electronic coupling and solvation can be clearly observed, and their effects on the electron-transfer rates quantitatively defined. These studies clearly indicate the factors that control the rates of nonradiative decay in radical ion pairs and thus the probabilities of observing other chemical and physical processes in these species.

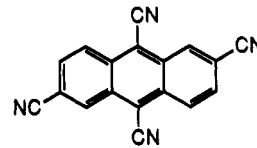
The main conclusions of the current work are similar to those described in a preliminary report.¹⁷ We have now determined, however, that the actinometry used previously to determine the quantum yields for free radical ion formation via excitation of the CT complexes was in error by a factor of ca. 2. In addition, we previously assumed that the rate of solvation of the CRIP to give the SSRIP was a constant for the systems studied. As detailed below, we now find that this is not the case. The combination of these two errors led, fortuitously, to estimates of return electron-transfer rates comparable to those reported in the current work. We regret these unfortunate errors!

Results and Discussion

The excited-state electron acceptors used in the present work are 9,10-dicyanoanthracene (DCA) and 2,6,9,10-tetracyanoanthracene (TCA). The donors are simple alkyl-substituted



DCA



TCA

benzenes (Table I). The selective formation of CRIP intermediates relies upon the formation of ground-state donor-acceptor complexes, as detailed later. TCA is clearly a better electron acceptor than DCA, and indeed for several of the donors in the presence of TCA, ground-state CT complex formation can be observed. These complexes have been characterized by using conventional methods as outlined in the following section.

(8) (a) Farid, S.; Hartman, S. E.; Evans, T. R. In *The Exciplex*; Gordon, M., Ware, W. R., Eds.; Academic Press: New York, 1975; p 327. (b) Arnold, D. R.; Wong, P. C. *J. Am. Chem. Soc.* **1979**, *101*, 1894. (c) Wong, P. C.; Arnold, D. R. *Can. J. Chem.* **1980**, *58*, 918. (d) Lewis, F. D. *Acc. Chem. Res.* **1979**, *12*, 152. (e) Lewis, F. D.; Simpson, J. T. *J. Phys. Chem.* **1979**, *83*, 2015. (f) Jones, G., In *Photoinduced Electron Transfer, Part A: Conceptual Basis*; Fox, M. A., Chanon, M., Eds.; Elsevier: Amsterdam, 1988; Chapter 1.7. (g) Miyashi, T.; Kamata, M.; Mukai, T. *J. Am. Chem. Soc.* **1987**, *109*, 2780. (9) (a) Czekalla, J.; Meyer, K.-O. Z. *Phys. Chem. Neue Folge* **1961**, *27*, 185. (b) Kobayashi, T.; Yoshihara, K.; Nagakura, S. *Bull. Chem. Soc. Jpn.* **1971**, *44*, 2603. (c) Prochorow, J.; Bernard, E. J. *Lumin.* **1974**, *8*, 471. (d) Rosenberg, H. M.; Eimutis, E. C. *J. Phys. Chem.* **1966**, *70*, 3494. See also: (e) Foster, R. *Organic Charge-Transfer Complexes*; Academic: New York, 1969; Chapter 3.B.

(10) (a) *The Exciplex*; Gordon, M., Ware, W. R., Eds.; Academic: New York, 1975. (b) Mattes, S. L.; Farid, S. *Acc. Chem. Res.* **1982**, *15*, 80. (c) Caldwell, R. A.; Creed, D. *Acc. Chem. Res.* **1980**, *13*, 45.

(11) Mataga, N.; Shioyama, H.; Kanda, Y. *J. Phys. Chem.* **1987**, *91*, 314.

(12) (a) Mataga, N.; Asahi, T.; Kanda, Y.; Okada, T.; Kakitani, T. *Chem. Phys.* **1988**, *127*, 249. (b) Asahi, T.; Mataga, N. *J. Phys. Chem.* **1989**, *93*, 6575.

(13) Ledwith, A. In *The Exciplex*; Gordon, M., Ware, W. R., Eds.; Academic Press: New York, 1975; p 209.

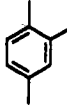
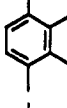
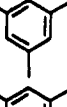
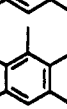
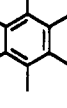
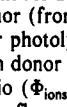
(14) (a) Gould, I. R.; Ege, D.; Mattes, S. L.; Farid, S. *J. Am. Chem. Soc.* **1987**, *109*, 3794. (b) Gould, I. R.; Moser, J. E.; Ege, D.; Farid, S. *J. Am. Chem. Soc.* **1988**, *110*, 1991. (c) Gould, I. R.; Farid, S. *J. Am. Chem. Soc.* **1988**, *110*, 7883. (d) Gould, I. R.; Moser, J. E.; Armitage, B.; Farid, S.; Goodman, J. L.; Herman, M. S. *J. Am. Chem. Soc.* **1989**, *111*, 1917.

(15) (a) Ohno, T.; Yoshimura, A.; Mataga, N. *J. Phys. Chem.* **1986**, *90*, 3296. (b) Ohno, T. *J. Phys. Chem.* **1985**, *89*, 5709. (c) Ohno, T.; Yoshimura, A.; Shioyama, H.; Mataga, N. *J. Phys. Chem.* **1987**, *91*, 4365. (d) Ohno, T.; Yoshimura, A.; Mataga, N.; Tazuke, S.; Kawanishi, Y.; Kitamura, N. *J. Phys. Chem.* **1989**, *93*, 3546. (e) Levin, P. P.; Pluzhnikov, P. F.; Kuzmin, V. A. *Chem. Phys. Lett.* **1988**, *147*, 283. (f) Vauthey, E.; Suppan, P.; Haselbach, E. *Helv. Chim. Acta* **1988**, *71*, 93. (g) Kikuchi, K.; Takahashi, Y.; Koike, K.; Wakamatsu, K.; Ikeda, H.; Miyasaka, T. *Z. Phys. Chem. (Wiesbaden)* **1990**, *167*, 27.

(16) (a) Marcus, R. A. *J. Chem. Phys.* **1965**, *43*, 679. (b) Marcus, R. A. *Faraday Discuss. Chem. Soc.* **1982**, *74*, 7.

(17) Gould, I. R.; Moody, R.; Farid, S. *J. Am. Chem. Soc.* **1988**, *110*, 7242.

TABLE I: Quantum Yields for Free Radical Ion Formation and Rate Constants for Return Electron Transfer for Solvent-Separated Radical Ion Pairs (SSRIP) and Contact Radical Ion Pairs (CRIP) of Tetracyanoanthracene (TCA) Radical Anion and Substituted Benzene Radical Cations in Acetonitrile at 25 °C (Subscripts ss and cp Refer to Data of the Solvent-Separated and Contact Pairs, Respectively)

donor	$E^{\text{ox}}_{\text{D}} - E^{\text{red}}_{\text{A}}^a$	$(\Phi_{\text{ions}})_{\text{ss}}^b$	$(k_{\text{et}})_{\text{ss}}^c$ 10^9 s^{-1}	$(\Phi_{\text{ions}})_{\text{cp}}^{d,e}$	$\Phi_{\text{solv}}^{e,f}$	$1/\tau_{\text{cp}}^{g,h}$ 10^9 s^{-1}	$k_{\text{solv}}^{e,h}$ 10^9 s^{-1}	$(k_{\text{et}})_{\text{cp}}^{e,i}$ 10^9 s^{-1}
	2.36	0.058 ^j	8.4	0.052	0.90	11.9	10.7	1.2
	2.28	0.042	11.4	0.020 (0.027)	0.47 (0.65)	9.3	4.4 (6.0)	4.9 (3.3)
	2.27	0.041	11.7	0.018	0.44	10.5	4.6	5.9
	2.22	0.041	11.7	0.016 (0.024)	0.39 (0.59)	10.4	4.1 (6.1)	6.3 (4.3)
	2.15	0.035	13.8	0.0063 (0.0036)	0.18 (0.10)	11.4	2.1 (1.1)	9.3 (10.3)
	2.03	0.031	15.8	0.0028	0.09	18.5	1.7	16.8

^aFrom ref 27. ^bQuantum yield for formation of free radical ions for photolysis of the acceptors at 410 nm, extrapolated to zero concentration of the donor (from ref 27). ^cCalculated by assuming $k_{\text{sep}} = 5 \times 10^8 \text{ s}^{-1}$, (ref 27; see also footnote 52). ^dQuantum yield for formation of free radical ions for photolysis of the CT complexes at 460 nm. ^eThe values in parentheses are based on data obtained from the dependence of the radical ion yield on donor concentration for excitation at 410 nm (see text). ^fYield of solvated radical ion pairs from contact radical ion pairs, determined from the ratio $(\Phi_{\text{ions}})_{\text{cp}}/(\Phi_{\text{ions}})_{\text{ss}}$ (cf. eq 3c). ^gThe lifetimes of the contact radical ion pairs (τ_{cp}) were obtained as the lifetimes of the exciplex/excited complex fluorescence. The TCA exciplexes with *m*-xylene, mesitylene, and *p*-xylene ($E^{\text{ox}}_{\text{D}} - E^{\text{red}}_{\text{A}} = 2.58, 2.55, \text{ and } 2.50 \text{ eV}$) gave $1/\tau_{\text{cp}}$ of $11.2 \times 10^9, 11.2 \times 10^9$ and $11.8 \times 10^9 \text{ s}^{-1}$. ^hObtained from the ratio $\Phi_{\text{solv}}/\tau_{\text{cp}}$. ⁱObtained from $(1 - \Phi_{\text{solv}})/\tau_{\text{cp}}$. ^jThe measured²⁷ Φ_{ions} (410-nm excitation) is 0.056. Correction was made to obtain $(\Phi_{\text{ions}})_{\text{ss}}$ since in this case diffusive quenching of $^1\text{TCA}^*$ leads to CRIP formation with ca. 25% efficiency.

A. Ground-State Complex Formation with TCA. Shown in Figure 1 is the absorption spectrum of TCA in acetonitrile at 25 °C. Upon addition of a donor, CT complex formation can be observed as a characteristic broad absorption above 450 nm and as a considerable decrease in the vibrational structure in the 350–420-nm region. This is illustrated in Figure 1 for the complex formed between TCA and pentamethylbenzene (PMB). The equilibria between the free acceptor (A) and the complex (AD), eq 1, formed between TCA and the donors durene, PMB, and



hexamethylbenzene (HMB), were analyzed according to the method of Benesi and Hildebrand.¹⁸ As expected, the equilibrium constants increasing as the oxidation potential of the donor decreases, i.e., with increasing ability to donate an electron. A plot of $\log K_{\text{CT}}$ vs the oxidation potential of the donor yields a straight line with a slope of -2.65 V^{-1} . For the TCA/PMB system a value of 3.2 M^{-1} was obtained for K_{CT} at 25 °C. K_{CT} was also determined at several temperatures between 10 and 40 °C for the TCA/PMB system. From these measurements, values of $-4.0 \pm 0.3 \text{ kcal mol}^{-1}$ and $-11 \pm 1 \text{ cal K}^{-1} \text{ mol}^{-1}$ were obtained for the enthalpy (ΔH) and entropy (ΔS) of complex formation. Such values are typical for these types of organic donors and acceptors.¹⁹

On the basis of the equilibrium constant of 3.2 M^{-1} , extrapolation of the spectrum to infinite PMB concentration allows an estimate of the absorption spectrum of the pure TCA/PMB complex, as illustrated by the dashed line in Figure 1. The spectrum is readily interpreted as consisting of two main absorption bands. A longer wavelength, broad featureless charge-transfer band overlaps a shorter wavelength band with diminished vibrational structure and somewhat reduced overall intensity, attrib-

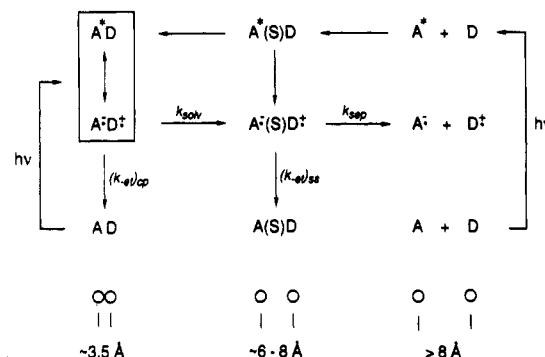


Figure 2. Intermediates involved in photoinduced electron-transfer reactions. The separation distance between the reactants increases from left to right. At contact the center-to-center separation of a pair of aromatic molecules in a face-to-face configuration is ca. 3.5 Å. In the solvent-separated configuration this distance increases to ca. 6–8 Å.¹ At larger distances the species are considered to be “free”. The energies of the species increase in the vertical direction from the ground neutral state to the ionic state to the locally excited state. The mixed state ($\text{A}^*\text{D} \leftrightarrow \text{A}^-\text{D}^+$) represents the general case of an exciplex/excited CT complex, which in the present case can be considered to be essentially a pure CRIP (A^-D^+). The horizontal arrows indicate reactions involving the movement of solvent molecules and change in solvation state. The vertical arrows indicate electron-transfer reactions. Excitation of a free molecular reactant (in this case A) to form the free locally excited state leads to ion-pair states upon encounter with a donor. Excitation of a ground-state CT complex leads to the CRIP directly.

utable to a perturbed locally excited band associated mainly with the TCA moiety. The absorption edges of the long-wavelength (CT) bands of the durene, PMB, and HMB complexes shift to lower energy by increments that are approximately equal to the decreases in the oxidation potentials of the donors.

B. Direct Formation of Contact and Solvent-Separated Radical Ion Pairs. The mechanistic scheme used in the present work is

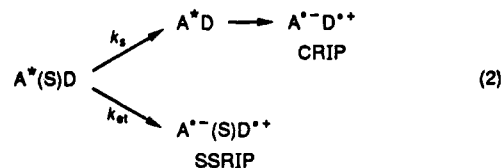
(18) Benesi, H. A.; Hildebrand, J. H. *J. Am. Chem. Soc.* **1949**, *71*, 2703.

(19) Foster, R. *Organic Charge-Transfer Complexes*; Academic: New York, 1969; Chapter 6.B.

shown in Figure 2 in which the various electronic states of the reactants are shown in contact, solvent-separated, and "free" configurations. In the contact configuration, mixing between locally excited (A^*D) and ion pair (A^+D^-) states must be considered. This is indicated in the figure by the exciplex (excited complex), $A^*D \leftrightarrow A^+D^-$, a limiting case of which is the contact radical ion pair (CRIP). As discussed below, the extent of charge separation in the exciplexes/excited CT complexes of the cyananthracene acceptors with the donors in Table I is high, so that it is valid to describe these species as essentially pure CRIP.

Excitation of ground-state CT complexes (AD, Figure 2) in the charge-transfer band is generally assumed to lead to CRIP formation directly, and indeed the results of the picosecond transient absorption spectroscopy in related systems confirm that the products of such excitation can be described as pure CRIP.^{11,12,20,21} In the present systems diffusion-controlled bimolecular quenching of a free excited-state acceptor (A^* , Figure 2) by a donor, D, however, may result in the direct formation of the SSRIP. The role of contact radical ion pairs, if any, in bimolecular electron-transfer quenching reactions in acetonitrile is not well understood. Weak CRIP (exciplex) emissions have been observed for some systems in acetonitrile; however, it is not generally known whether the emissions are weak because the CRIP radiative rates in acetonitrile are small (leading to a small emission probability)²² or because the CRIP is bypassed in a quenching event that leads directly to the SSRIP.²³ We have observed weak exciplex emissions in the case of quenching of excited DCA by several of the current donors in acetonitrile,²⁴ which indicates that for this acceptor at least, some contact radical ion pairs are formed as a result of the bimolecular quenching process in this solvent. In fact, a systematic evaluation of their radiative rate constants indicates that these exciplexes are formed with high efficiency.²⁴ After extensive purification of TCA we have been able to conclusively assign very weak emissions ($\Phi < 10^{-4}$) to exciplexes/excited complexes of this acceptor with the alkylbenzene donors in acetonitrile.²⁵ From the dependence of these exciplex emissions on the donor concentration we observed a dramatic variation in the efficiency of CRIP formation in the diffusive quenching of $^1TCA^*$ by the different donors. With the weak donors such as *m*-xylene and mesitylene, the exciplexes are formed with high efficiency (larger than 0.7 and probably close to unity). On the other hand, with the strong donors including durene, PMB, and HMB, the exciplex fluorescence is observed to increase with increasing concentration of the donor in a manner consistent with formation of the exciplexes exclusively through direct excitation of the ground-state complex, with diffusive quenching leading to CRIP formation with low or zero efficiency in these cases.²⁶ 1,2,4-Trimethylbenzene, which has an oxidation potential between those of mesitylene and durene, shows intermediate behavior; diffusive quenching in this case leads to CRIP formation with ca. 25% efficiency.²⁶ The CRIP formation efficiency appears to

decrease as the driving force for the ion-pair-forming electron-transfer reaction increases (i.e., as the oxidation potential of the donor decreases) which is consistent with these reactions being in the Marcus "normal" region.²⁶ To "bypass" the CRIP, electron-transfer quenching must occur from the donor (D) to the excited acceptor (A^*) in the encounter pair ($A^*(S)D$) before its "collapse" to produce A^* and D in contact and hence a CRIP (k_{-1} , eq 2). The encounter pair is understood to be a dynamic structure



with the reactants in a "loose" (solvent-separated) configuration, within which electron transfer can take place. The observation that the CRIP formation efficiency varies from near unity to almost zero by changing the donor from *m*-xylene to durene suggests that the rate of the SSRIP forming reaction in the encounter pair increases by more than 2 orders of magnitude as the exothermicity²⁷ of this reaction increases from 0.3 to 0.65 eV. This steep dependence of the electron-transfer rate on the driving force indicates that the reorganization energy for this process is considerably larger than 0.6 eV. We have previously estimated the total reorganization energy to be ca. 1.9 eV for electron-transfer reactions in solvent-separated radical-ion pairs.²⁷ This value is significantly larger than the exothermicities of the charge separation reactions discussed here, and so it is quite reasonable that the rate of the SSRIP-forming process changes with driving force in the manner observed.²⁸

C. Quantum Yields of Free Ion Formation. Quenching of free excited TCA by the low oxidation potential donors leads directly to SSRIP. Quenching of free excited TCA by the higher oxidation potential donors or of free excited DCA by any of the donors results in the formation of CRIP. However, in these latter cases the return electron-transfer reactions are exothermic by more than 2.5 eV. As indicated in section D, the rates of the return electron-transfer reactions in CRIP with such exothermicities are much smaller than the rates of solvation of the CRIP to form SSRIP. Thus, the quantum yields for formation of free radical ions via diffusive quenching of either acceptor provide information concerning the competing reactions of the SSRIP only. According to Figure 2 the quantum yield for formation of free radical ions from an SSRIP is given by eq 3a. From such quantum yield measurements we have previously been able to determine values for the return electron-transfer rate constants in the SSRIP, (k_{-et})_{ss.²⁷} The return electron-transfer rates for the corresponding CRIP, (k_{-et})_{cp, can be obtained by using an extension of this quantum yield method as described below.³⁰}

(27) Gould, I. R.; Ege, D.; Moser, J. E.; Farid, S. *J. Am. Chem. Soc.* **1990**, *112*, 4290.

(28) These conclusions are consistent with the work of Mataga et al.^{11,12b} and Jones et al.,²⁹ who have reported that different types of radical ion pair can be formed as a result of excitation of free donors or acceptors and their corresponding CT complexes.

(29) (a) Jones, G., II; Becker, W. G. *J. Am. Chem. Soc.* **1982**, *104*, 271. (b) Jones, G., II; Becker, W. G. *J. Am. Chem. Soc.* **1981**, *103*, 4630. (c) Jones, G., II; Becker, W. G. *J. Am. Chem. Soc.* **1983**, *105*, 1276. (d) Jones, G., II; Malba, V. *Chem. Phys. Lett.* **1985**, *119*, 105. (e) Jones, G., II; Haney, W. A.; Phan, X. T. *J. Am. Chem. Soc.* **1988**, *110*, 1922.

(30) The experimental details of the ion yield method are described in ref 27. In the present work we used 4-methoxystilbene (MS) instead of 4,4'-dimethoxystilbene (DMS) as a low-oxidation-potential monitor for the free-radical cations. When DMS was used to monitor the low ion yields from CT excitation, there was observed, in addition to the fast scavenging of the free radical cations, a further scavenging reaction on a slower time scale. We attribute this to electron-transfer quenching of free excited triplet TCA formed in a very low yield via intersystem crossing in the CRIP, which becomes noticeable only when the overall quantum yield for free ion formation is also very low. The triplet state scavenging, however, was not observed when MS was used. This is readily understood since the rate of the reaction of $^1TCA^*$ with DMS yielding DMS^{•+} is slower than diffusion controlled, and thus the corresponding reaction rate with MS, which is 0.15 eV more endothermic due to the higher oxidation potential of this stilbene derivative, must be significantly reduced.

(20) (a) Goodman, J. L.; Peters, K. S. *J. Am. Chem. Soc.* **1985**, *107*, 1441. (b) Goodman, J. L.; Peters, K. S. *J. Phys. Chem.* **1986**, *90*, 5506. (c) Goodman, J. L.; Peters, K. S. *J. Am. Chem. Soc.* **1985**, *107*, 6459. (d) Goodman, J. L.; Peters, K. S. *J. Am. Chem. Soc.* **1986**, *108*, 1700. (e) Peters, K. S.; Angel, S. A.; O'Driscoll, E. *Pure Appl. Chem.* **1989**, *61*, 629.

(21) (a) Hilinski, E. F.; Masnovi, J. M.; Amatore, C.; Kochi, J. K.; Rentzepis, P. M. *J. Am. Chem. Soc.* **1983**, *105*, 6167. (b) Hilinski, E. F.; Masnovi, J. M.; Kochi, J. K.; Rentzepis, P. M. *J. Am. Chem. Soc.* **1984**, *106*, 8071. (c) Masnovi, J. M.; Kochi, J. K.; Hilinski, E. F.; Rentzepis, P. M. *J. Am. Chem. Soc.* **1986**, *108*, 1126.

(22) (a) Mataga, N.; Okada, T.; Yamamoto, N. *Chem. Phys. Lett.* **1967**, *1*, 119. (b) Mataga, N.; Murata, Y. *J. Am. Chem. Soc.* **1969**, *91*, 3144.

(23) Knibbe, H.; Röllig, K.; Schäfer, F. P.; Weller, A. *J. Chem. Phys.* **1967**, *47*, 1184.

(24) Farid, S.; Gould, I. R.; Young, R. H., unpublished results. The full details of these experiments will be reported elsewhere.

(25) Support for assigning these weak emissions to TCA exciplexes is provided by the observation that the emission maxima shift to longer wavelength with decreasing donor oxidation potential and correlate well with those of the DCA exciplexes in acetonitrile. Further support comes from the observed deuterium isotope effects on the emission lifetimes (section E and Table II), which agree well with the isotope effects observed for the ion yields.

(26) Gould, I. R.; Mueller, L. J.; Farid, S. *Z. Phys. Chem. (Wiesbaden)*, submitted.

Efficient ground-state CT complex formation is observed with TCA and the lower oxidation potential donors. Due to their different absorbances, it is possible to excite either the free or complexed TCA by adjusting the excitation wavelength and/or the concentration of the donor. Excitation of the complexed TCA results in formation of a CRIP ($A^{\cdot-}D^{+\cdot}$), which might undergo return electron transfer to re-form the neutral starting materials ($(k_{-et})_{cp}$), or solvation to form a solvent-separated radical ion pair ($A^{\cdot-}(S)D^{+\cdot}$), (k_{solv}). According to Figure 2, the quantum yields for free-radical ion formation are thus different in these systems for excitation via the two pathways if the return electron-transfer step ($k_{-et})_{cp}$ can compete with solvation, k_{solv} . The quantum yields for free radical ion formation via excitation of the free acceptor ($(\Phi_{ions})_{ss}$) and for excitation of the CT complex ($(\Phi_{ions})_{cp}$) are given by eq 3. $(\Phi_{ions})_{cp}$ is given by the product of the yield of SSRIP

$$(\Phi_{ions})_{ss} = \frac{k_{sep}}{k_{sep} + (k_{-et})_{ss}} \quad (3a)$$

$$\Phi_{solv} = \frac{k_{solv}}{k_{solv} + (k_{-et})_{cp}} \quad (3b)$$

$$(\Phi_{ions})_{cp} = \Phi_{solv}(\Phi_{ions})_{ss} \quad (3c)$$

formed from the CRIP via the solvation process, Φ_{solv} (eq 3b), and the yield of free ions from the SSRIP, $(\Phi_{ions})_{ss}$, eq 3c. The quantum yield $(\Phi_{ions})_{cp}$ can be obtained directly from experiments performed in the presence of high concentrations of donor by excitation into the CT band at 460 nm (Figure 1). At wavelengths less than 450 nm, both the free TCA and the complex absorb, and thus the quantum yield for excitation at these wavelengths (λ) will depend upon the concentration of D, since this changes the equilibrium concentrations of TCA and complex, and thus the partition of the excitation light into these two species. At lower concentrations of D, less TCA will be complexed, and the observed quantum yield, corrected for incomplete interception of the excited acceptor, $(\Phi_{ions})_{\lambda}$, will approach that shown in eq 3a. At higher concentrations of D, more TCA will be complexed and the quantum yield will approach that of eq 3c. When both the free and complexed TCA absorb the excitation light, the quantum yield is given by eq 4a, in which ϵ_{AD} and ϵ_A are the extinction coefficients

$$\frac{1}{(\Phi_{ions})_{\lambda}} = \frac{1}{(\Phi_{ions})_{ss}} \frac{1 + \left(\frac{\epsilon_{AD}}{\epsilon_A}\right)_{\lambda} K_{CT}[D]}{1 + \Phi_{solv} \left(\frac{\epsilon_{AD}}{\epsilon_A}\right)_{\lambda} K_{CT}[D]} \quad (4a)$$

$$\frac{1}{(\Phi_{ions})_{410}} = \frac{1}{(\Phi_{ions})_{ss}} \frac{1 + K_{CT}[D]}{1 + \Phi_{solv} K_{CT}[D]} \quad (4b)$$

$$\frac{1}{(\Phi_{ions})_{460}} = \frac{1}{(\Phi_{ions})_{ss}} \frac{1}{\Phi_{solv}} \quad (4c)$$

of the complex and the free acceptor at the excitation wavelength, λ . According to Figure 1, there is an isosbestic point at 410 nm for the TCA/PMB system. Indeed, for all of the donors used in the present study with TCA, at all concentrations, an isosbestic point is observed close to this wavelength. Thus at 410 nm, ϵ_A is equal to ϵ_{AD} and eq 4a simplifies to eq 4b. At 460 nm, ϵ_A is negligible and eq 4a reduces to eq 4c, which is equivalent to eq 3c since $(\Phi_{ions})_{460}$ is equal to $(\Phi_{ions})_{cp}$. We have analyzed the TCA/PMB system as a function of concentration according to eq 4 at two different wavelengths.

Quantum yields for free radical ion formation were measured for excitation of TCA at 410 nm, as a function of PMB concentration. In Figure 3 the quantum yield data are plotted as $1/(\Phi_{ions})_{410}$ versus the concentration of PMB. From this plot a value of 0.035 was determined for $(\Phi_{ions})_{ss}$ by extrapolation to zero concentration of PMB. The curve through the data points for 410 nm excitation in Figure 3 was calculated according to eq 4b using 3.2 M^{-1} for K_{CT} and a value of 0.1 for Φ_{solv} , which gave the best fit to the data.

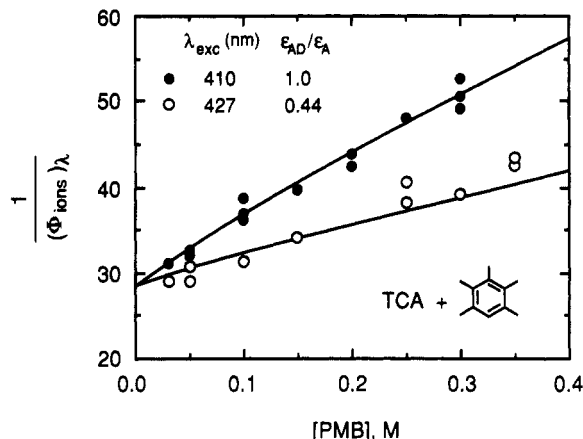


Figure 3. Plots of reciprocal quantum yield for formation of free radical ions for photolysis (in acetonitrile at 25 °C) of TCA in the presence of PMB, as a function of PMB concentration. The closed circles refer to photolysis at 410 nm, and the open circles refer to photolysis at 427 nm. The curves are based on calculations according to eq 4 with the parameters given in the text.

At 427 nm, an absorption maximum of TCA, the extinction coefficient of the complex is approximately 0.44 times that of the free TCA (Figure 1). Thus, according to eq 4a, we expect a different concentration dependence for the quantum yield at this wavelength. Also shown in Figure 3 is the reciprocal of the quantum yield at this wavelength as a function of PMB concentration. A good fit to these data can be obtained using eq 4a with the same values for the parameters $(\Phi_{ions})_{ss}$, Φ_{solv} and K_{CT} used to fit the 410 nm data, and 0.44 for the ratio ϵ_{AD}/ϵ_A . The slight deviation between the measured and calculated quantum yields at high concentrations of PMB is probably due to a reduction in the extinction coefficient of the free TCA resulting from changes in the bulk solvent properties as the concentration of the hydrocarbon increases. Support for this explanation comes from the observation that the optical density at 427 nm of a solution of TCA in acetonitrile decreases by ca. 8% upon the addition of 0.3 M benzene. A decrease in the extinction coefficient at this wavelength results in a higher ratio of excited complexed to free TCA (higher $(\epsilon_{AD}/\epsilon_A)_{\lambda}$) and thus a correspondingly lower $(\Phi_{ions})_{\lambda}$.

The $(\Phi_{ions})_{ss}$ were obtained for all of the donors of Table I with TCA by extrapolation of the $(\Phi_{ions})_{410}$ to zero donor concentration as outlined above. Estimates for Φ_{solv} were obtained by fitting the yield versus concentration data as described above. Values for $(\Phi_{ions})_{cp}$ were also obtained for each donor by excitation of the corresponding CT complexes at 460 nm. Absolute quantum yields for free radical ion formation for 460-nm excitation were obtained by using relative actinometry with the 410-nm experiments as detailed in the Experimental Section. From these experiments, values of Φ_{solv} could then be determined for each system by using eq 3c (Table I). In several cases somewhat different values were obtained for Φ_{solv} from the 410 and the 460-nm experiments (Table I). The origin of these differences, which seem to be greater than the expected experimental error, is not clear.

In a series of interesting papers on the photochemistry of ground-state charge-transfer complexes, Jones et al. observed that in some systems the quantum yields of chemical product formation were lower for excitation at longer wavelengths in the CT band compared to excitation at shorter wavelengths.^{8f,29} These observations were rationalized as being due to the formation of vibrationally excited charge-transfer states. In the present cases, however, there is no clear evidence for the decreased free ion quantum yield with longer wavelength excitation.

D. Determination of Solvation and Return Electron-Transfer Rate Constants. From the $(\Phi_{ions})_{ss}$ and Φ_{solv} data summarized in Table I, values for $(k_{-et})_{ss}$ and $(k_{-et})_{cp}$ can thus be determined by using eqs 3a and 3b, if values can be obtained for k_{sep} and k_{solv} . The rate constant k_{sep} has not been measured directly in these systems, but a value of $5 \times 10^8 \text{ s}^{-1}$ has been estimated previously for related SSRIP in acetonitrile.²⁷ Thus, the $(k_{-et})_{ss}$ summarized

in Table I were obtained by assuming this value to be a constant for all of the SSRIP.

Estimates for k_{solv} can be obtained from the photophysical behavior of the exciplexes. The important decay processes for exciplexes are nonradiative decay, in the present case by return electron transfer to the ground (neutral) state, $(k_{\text{et}})_{\text{cp}}$, radiative decay to the ground (neutral) state, and solvation to form the solvent-separated radical ion pair. Other possible decay processes include reverse formation of the excited-state acceptor and donor, chemical reaction, and intersystem crossing; however, none of these are important in the present cases in acetonitrile.²⁴ The emission quantum yields are small (ca. $(2-5) \times 10^{-3}$ for the DCA exciplexes and an order of magnitude lower for those of TCA), and thus the exciplex decays are dominated by nonradiative processes. We have found that in other solvents, the rates of nonradiative decay to the ground state in these exciplexes depend upon the redox properties of the donors and acceptors due to the energy-gap effect.²⁴ However, the measured lifetimes of the DCA exciplexes (contact pairs), τ_{cp} , in acetonitrile are 1.6, 1.9, and 1.8 ns for durene, PMB, and HMB and thus do not appear to depend upon the donor oxidation potential. This can be explained if the return electron-transfer processes are slow compared to another, energy-gap-independent, nonradiative process. In acetonitrile this is most likely to be solvation to form the SSRIP. Therefore, the reciprocal of the average of the lifetimes, $6 \times 10^8 \text{ s}^{-1}$, is taken as an estimate for the solvation rates of these exciplexes, k_{solv} .³¹

The lifetimes of the TCA exciplexes (contact pairs), τ_{cp} , are given in Table I. Surprisingly, these lifetimes are more than an order of magnitude smaller than those of the DCA exciplexes mentioned above, even when the return electron-transfer free energies are similar (vide infra). Moreover, the lifetimes of the TCA exciplexes with the higher oxidation potential donors *m*-xylene, *p*-xylene, mesitylene, and 1,2,4-trimethylbenzene are almost equal (84–89 ps). The Φ_{solv} for the CRIP of TCA/1,2,4-trimethylbenzene is ca. 0.9 (Table I), indicating that return electron transfer is slow compared to solvation to form a SSRIP, which thus represents the major decay process for this exciplex. In this case, therefore, k_{solv} is given approximately by the reciprocal of the exciplex lifetime. For the higher oxidation potential tri- and disubstituted donors, the rate of return electron transfer will be even smaller than for 1,2,4-trimethylbenzene due to the inverted region effect, as detailed later. Thus, for these exciplexes the rates of solvation, k_{solv} , are essentially the reciprocals of the exciplex lifetimes, i.e., ca. $1.1 \times 10^{10} \text{ s}^{-1}$. For the lower oxidation potential donors Φ_{solv} is less than unity, which suggests that return electron transfer becomes significant in these exciplexes. In these cases k_{solv} can be estimated from the ratio $\Phi_{\text{solv}}/\tau_{\text{cp}}$, eq 3b, where τ_{cp} is assumed to be given by $1/(k_{\text{solv}} + (k_{\text{et}})_{\text{cp}})$. For the case of HMB, for example, Φ_{solv} is only 0.09, which gives a value of $1.7 \times 10^9 \text{ s}^{-1}$ for k_{solv} (Table I). Therefore, as indicated in Table I, and contrary to our previous assumption,¹⁷ k_{solv} appears not to be constant, even for these systems that have closely related structures. This unexpected finding might be explained by differences in the relative energies of the CRIP and the corresponding SSRIP as a function of the donor substitution pattern or oxidation potential. Indeed a rough trend can be discerned for the data in Table I in that k_{solv} is ca. $2 \times 10^9 \text{ s}^{-1}$ for the CRIP of PMB and HMB, is ca. $4 \times 10^9 \text{ s}^{-1}$ for the three different tetramethylbenzenes, and reaches ca. $1.1 \times 10^{10} \text{ s}^{-1}$ for the tri- and disubstituted benzenes.

On the basis of the relationship between oxidation potential E^{ox} and gas-phase ionization potential IP, Kochi et al.³² suggested that the solvent stabilization of the alkylbenzene radical cations might depend upon the substitution pattern. From their data in trifluoroacetic acid these parameters are empirically related according to $E^{\text{ox}} = \text{IP} - C$, in which a component of the constant C is the free energy associated with solvation (ΔG_s°). C was found

TABLE II: Deuterium Isotope Effects on Quantum Yields of Free Ion Formation and Rate Constants for Return Electron Transfer for Solvent-Separated Radical Ion Pairs and Contact Radical Ion Pairs of Tetracyanoanthracene Radical Anions and Substituted Benzene Radical Cations in Acetonitrile

donor	$(\Phi_{\text{ions}}^{\text{d}})_{\text{cp}}/(\Phi_{\text{ions}}^{\text{h}})_{\text{cp}}^a$	$(\Phi_{\text{ions}}^{\text{d}})_{\text{ss}}/(\Phi_{\text{ions}}^{\text{h}})_{\text{ss}}^b$	$\Phi_{\text{solv}}^{\text{d}}/\Phi_{\text{solv}}^{\text{h}}^c$	$\tau_{\text{cp}}^{\text{d}}/\tau_{\text{cp}}^{\text{h}}^c$	$(k_{\text{et}}^{\text{h}})_{\text{cp}}/(k_{\text{et}}^{\text{d}})_{\text{cp}}^a$	$(k_{\text{et}}^{\text{h}})_{\text{ss}}/(k_{\text{et}}^{\text{d}})_{\text{ss}}^b$
durene	1.58	1.20	1.32	1.36	1.66	1.21
hexamethylbenzene	1.59	1.10	1.45	1.55	1.52	1.10

^a Based upon the quantum yield of free radical ion formation upon excitation at 460 nm (Table I). ^b Data from ref 14c. ^c From the emission lifetimes of the appropriate CRIP.

to be different for the differently substituted benzenes, being $6.15 \pm 0.04 \text{ eV}$ for the di- and trisubstituted benzenes, $6.02 \pm 0.05 \text{ eV}$ for the tetramethylbenzenes, and $5.96 \pm 0.03 \text{ eV}$ for PMB and HMB. These results suggest that relative to the gas phase, the di- and trisubstituted derivatives are more stabilized by solvation by ca. 0.19 eV, and the tetrasubstituted derivatives by ca. 0.06 eV, compared to the penta- and hexasubstituted analogues. The radical ions will be less solvated in the CRIP than the SSRIP, and thus the step from CRIP to SSRIP may be somewhat more exothermic for the benzenes with fewer methyl substituents, leading to an increased k_{solv} . The lifetime data also suggest that the rates of solvation of the CRIP of DCA are significantly slower than the corresponding rates for the CRIP of TCA. This observation may also be due to differences in solvation of the two radical anions in the ion pairs, although clearly the factors that control these solvation rates are not well understood.

Whatever the reason for the observed differences in k_{solv} , the return electron-transfer rate $(k_{\text{et}})_{\text{cp}}$ can be determined from the measured lifetimes of the CRIP fluorescence, $1/(k_{\text{solv}} + (k_{\text{et}})_{\text{cp}})$, and the corresponding Φ_{solv} by using eq 3b. The values for $(k_{\text{et}})_{\text{cp}}$ obtained in this way, Table I, clearly decrease with increasing exothermicity as expected for reactions in the Marcus inverted region.²⁷

E. Isotope Effects on Return Electron-Transfer Rate Constants. In a previous study on $(k_{\text{et}})_{\text{ss}}$ it was found that the rates were decreased by substitution of deuterium for hydrogen in several of the donors in Table I.^{14c} The isotope effect was specific to substitution on the methyl groups and the magnitude was related to the reaction exothermicity. These observations were taken as evidence for quantum effects on the electron-transfer reactions. To further the investigations along these lines, isotope effects were sought for the $(k_{\text{et}})_{\text{cp}}$. The quantum yields $(\Phi_{\text{ions}})_{\text{ss}}$ and $(\Phi_{\text{ions}})_{\text{cp}}$ were measured for TCA with durene-*d*₁₄ and HMB-*d*₁₈ by using the methods described above (Table II). From these data the isotope effects on $(k_{\text{et}})_{\text{ss}}$ and $(k_{\text{et}})_{\text{cp}}$ were obtained as summarized in Table II. In the present study we are not able to examine the dependence of $(k_{\text{et}}^{\text{h}}/k_{\text{et}}^{\text{d}})_{\text{cp}}$ on the reaction exothermicity due to the small number of available CT complexes. The isotope effects on $(k_{\text{et}})_{\text{cp}}$, however, are in qualitative agreement with those on $(k_{\text{et}})_{\text{ss}}$ and are in fact considerably larger in magnitude.

F. Theoretical Treatment of Thermal and Radiative Electron-Transfer Data. Electron-transfer rate data are frequently analyzed by using a golden rule type formula such as eq 5.³³ A

$$k_{\text{et}} = \sum_{j=0}^{\infty} F_j V^2 \left(\frac{4\pi^2}{h^2 \lambda_s k_B T} \right)^{1/2} \exp \left[-\frac{(j h \nu_v + \Delta G_{\text{et}} + \lambda_s)^2}{4 \lambda_s k_B T} \right] \quad (5a)$$

$$F_j = e^{-S} S^j / j! \quad (5b)$$

$$S = \lambda_v / h \nu_v \quad (5c)$$

(31) The lifetimes of these exciplexes are similar to the lifetime of ca. 2 ns reported previously for the pyrene/dimethylaniline system in acetonitrile.^{1b,2c}

(32) Howell, J. O.; Goncalves, J. M.; Amatore, C.; Klasinc, L.; Wightman, R. M.; Kochi, J. K. *J. Am. Chem. Soc.* **1984**, *106*, 3968.

(33) (a) Hopfield, J. J. *Proc. Natl. Acad. Sci. U.S.A.* **1974**, *71*, 3640. (b) Van Duyne, R. P.; Fischer, S. F. *Chem. Phys.* **1974**, *5*, 183. (c) Ulstrup, J.; Jortner, J. *J. Chem. Phys.* **1975**, *63*, 4358. (d) Siders, P.; Marcus, R. A. *J. Am. Chem. Soc.* **1981**, *103*, 741, 748. (e) Marcus, R. A. *J. Chem. Phys.* **1984**, *81*, 4494. (f) Marcus, R. A.; Sutin, N. *Biochim. Biophys. Acta* **1985**, *811*, 265.

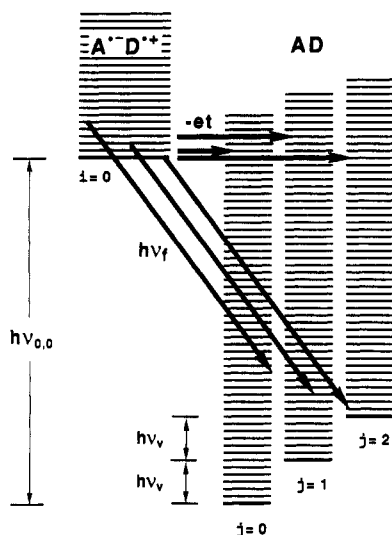


Figure 4. Origin and relationship of the golden rule formulas for non-radiative return electron transfer, $-et$, eq 5, and charge-transfer fluorescence ($h\nu_f$), eq 6. It is assumed that only one internal vibrational mode of frequency ν_v is active (i.e., suffers reorganization). In the initial, ionic state (A^+D^{*+}), there are i quanta in this mode; in the final, neutral (AD) state, there are j quanta. Assuming that $h\nu_v \gg k_B T$, only the $i = 0$ mode is initially occupied, whereas various final vibrational states (j) may be formed. Associated with each vibronic state is a stack of sublevels representing low-frequency ($\ll k_B T/h$) modes (e.g., solvent rotation). Return electron transfer or charge-transfer fluorescence is a composite of many individual transitions, all involving the same energy change (0 or $-h\nu_f$) between sublevels of the initial and final states. The rates of the individual transitions are proportional to thermal-occupation and Franck-Condon factors which are the same for return electron transfer and charge-transfer fluorescence except that different portions of the final-state spectrum are selected by the energy-matching condition. By observing fluorescence at various frequencies ν_f , one interrogates various final states. One does the same by measuring k_{-et} over a series of related donors or acceptors whose overall electron-transfer reaction exothermicities vary.

schematic representation of the electron-transfer process according to this model is shown in Figure 4. In eq 5, V is the magnitude of an electronic matrix element between the initial and final states, in this case those of the radical ion pair and the neutral molecules. ΔG_{-et} is the reaction free energy for return electron transfer. High-frequency ($\gg k_B T/h$) skeletal vibrations of the donor and acceptor are represented by a single "average" mode (the v mode), with a fixed frequency, ν_v , and reorganization energy, λ_v , which is associated with changes in the nuclear positions of the species undergoing electron transfer. Low-frequency ($\ll k_B T/h$) motions such as reorientation of the solvent and, perhaps, low-frequency skeletal vibrations or relative motions (librations) of the donor and acceptor have a reorganization energy λ_s . Each summand in eq 5 represents the rate for a single contribution to the total rate from a $0 \rightarrow j$ nonradiative vibronic transition (Figure 4). The corresponding Franck-Condon factors for the v mode are given by eqs 5b and 5c. The vibronic transitions are accompanied by energy-conserving transitions of the low-frequency modes. The probability that these modes accept the necessary energy involves further Franck-Condon, energy conservation, and thermal weighting factors for the various states of these modes. When summed, these result in the factors following V^2 in eq 5a.

In previous studies of return electron transfer within SSRIP, a value for λ_v was obtained from a simple analysis of the CT absorption and emission spectra of a TCA complex, and ν_v was assumed to be 1500 cm^{-1} for consistency with other work.³⁴⁻³⁸

(34) (a) Closs, G. L.; Johnson, M. D.; Miller, J. R.; Piotrowski, P. *J. Am. Chem. Soc.* **1989**, *111*, 3751. (b) Closs, G. L.; Miller, J. R. *Science* **1988**, *240*, 440. (c) Closs, G. L.; Calcaterra, L. T.; Green, N. J.; Penfield, K. W.; Miller, J. R. *J. Phys. Chem.* **1986**, *90*, 3673. (d) Miller, J. R.; Calcaterra, L. T.; Closs, G. L. *J. Am. Chem. Soc.* **1984**, *106*, 3047.

(35) (a) Miller, J. R.; Beitz, J. V.; Huddleston, R. K. *J. Am. Chem. Soc.* **1984**, *106*, 5057. (b) Miller, J. R.; Beitz, J. V. *J. Chem. Phys.* **1981**, *74*, 6476. (c) Beitz, J. V.; Miller, J. R. *J. Chem. Phys.* **1979**, *71*, 4579.

Values for λ_s and V were obtained by curve fitting eq 5 to a plot of $(k_{-et})_{ss}$ versus ΔG_{-et} .²⁷ For the $(k_{-et})_{cp}$ data the range of ΔG_{-et} is insufficient to allow accurate estimates of these parameters in this way. Furthermore, the assumptions by which the ΔG_{-et} were obtained for the SSRIP from electrochemical measurements on the donors and acceptors are not necessarily valid for the CRIP (vide infra). Therefore, we sought a method to obtain independent estimates for the reorganization parameters, for V , and for ΔG_{-et} of the CRIP.

It is well-known that there is a close relationship between thermal electron transfer and radiative charge-transfer spectra,³⁹ as illustrated schematically in Figure 4. The intensity of emission (photons per molecule per unit time per unit spectral energy) is given by eq 6,^{39a} which is formally very similar to the expression

$$I(\nu) = \left[n \left(\frac{n^2 + 2}{3} \right)^2 \right] \left(\frac{16\pi^2}{3} \bar{\nu}_f^3 \right) \times \sum_{j=0}^{\infty} F_j M^2 \left(\frac{4\pi^3}{h^2 \lambda_s k_B T} \right)^{1/2} \exp \left[- \frac{(j h \nu_v + \Delta G_{-et} + \lambda_s + h \nu_f)^2}{4 \lambda_s k_B T} \right] \quad (6)$$

for the electron-transfer rate, eq 5. Here M is the magnitude of the electronic transition moment (dipole length form), ν_f is the frequency, and $h\nu_f$ is the energy of the emitted photon. In a simple model, M is related to the matrix element V , the energy of maximum emission intensity $(h\nu_f)_{max}$, and the static dipole moment of the ion pair state μ_{cp} , as shown in eq 7.⁴⁰ Finally, n is the

$$M = V \mu_{cp} / (h\nu_f)_{max} \quad (7)$$

refractive index of the solvent whose effect on the intensity is represented by the prefactor in brackets.⁴¹ Thus, an analysis of the CRIP emission spectra of TCA according to eq 6 would provide an independent method for evaluating the parameters of eq 5. Whereas emission from TCA/alkylbenzene exciplexes (CRIP) can be detected in nonpolar and medium-polarity solvents, as discussed earlier, emission from the CRIP of TCA in acetonitrile is too weak for analysis according to eq 6. However, stronger exciplex emission can be observed in acetonitrile by using DCA as the acceptor with donors such as durene, PMB, and HMB. From studies of DCA and TCA exciplex emissions in various solvents, we have found that the electronic structures of these DCA exciplexes in acetonitrile are essentially pure CRIP, i.e., with only minor admixtures of other states.⁴² Thus the DCA exciplexes represent good model systems for the CRIP of TCA in acetonitrile and were analyzed according to eq 6.²⁴

G. Fitting of CRIP Radiative Electron-Transfer Spectra. Unlike the rate data for nonradiative return electron transfer, enough of the energy dependence of the radiative return electron-transfer process is known from the emission spectrum that accurate estimates can be made for the various fitting parameters. Shown in Figure 5 is the emission spectrum of the DCA/PMB exciplex in acetonitrile together with the fit to this spectrum using eq 6. In acetonitrile, reorganization of the solvent represents a large contribution to the total reorganization energy, and in this solvent it is possible to find a range of the parameters ΔG_{-et} , λ_s , λ_v , and ν_v that gives good fits to the emission spectrum. In less

(36) Gunner, M. R.; Robertson, D. E.; Dutton, P. L. *J. Phys. Chem.* **1986**, *90*, 3783.

(37) Kemnitz, K. *Chem. Phys. Lett.* **1988**, *152*, 305.

(38) The deuterium isotope effects^{14c} suggest that high-frequency carbon-hydrogen modes might be involved. However, deuterium substitution will also influence lower frequency carbon-carbon skeletal modes, and so no clear conclusions can yet be drawn from these experiments concerning the selection of the appropriate ν_v .

(39) (a) Marcus, R. A. *J. Phys. Chem.* **1989**, *93*, 3078 and references therein. (b) For a recent example see: Penfield, K. W.; Miller, J. R.; Padon-Row, M. N.; Cotsaris, E.; Oliver, A. M.; Hush, N. S. *J. Am. Chem. Soc.* **1987**, *109*, 5061.

(40) Cannon, R. D. *Electron transfer reactions*; Butterworths: Boston, 1980; Section 8.3.

(41) Knoester, J.; Mukamel, S. *Phys. Rev. A* **1989**, *40*, 7065.

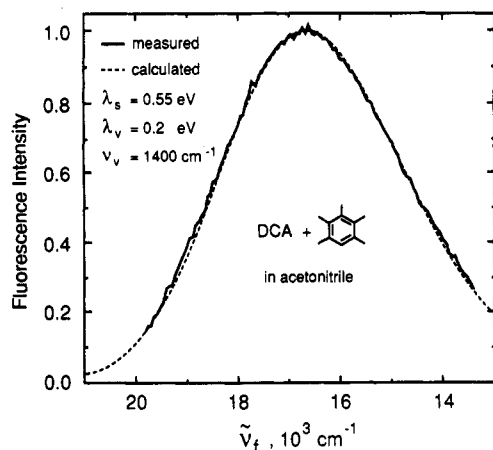


Figure 5. Emission spectrum of the DCA/PMB exciplex in acetonitrile at room temperature. The dashed line represents the fit to the spectrum obtained by using eq 6 with $\lambda_s = 0.55$ eV, $\lambda_v = 0.20$ eV, $\nu_v = 1400$ cm^{-1} , and $(\Delta G_{-et})_{cp} = -2.67$ eV.

polar solvents, however, the rearranged high-frequency mode becomes more dominant, and the fitting is more critical. Under these conditions, with TCA exciplexes, the best values for λ_v and ν_v are 0.18–0.20 eV and 1300–1400 cm^{-1} , respectively.²⁴ Fixing λ_v and ν_v at 0.20 eV and 1400 cm^{-1} , the values for λ_s and $(\Delta G_{-et})_{cp}$ that best fit the DCA/PMB emission spectrum in acetonitrile are 0.55 and -2.67 eV. The values for λ_v and ν_v are both slightly smaller than those we have used in the past (0.25 eV, 1500 cm^{-1});²⁷ however, the current values should be more accurate.

It is not trivial to extract V from the overall intensity of emission (or the fluorescence rate constant, k_f) by using an expression such as eq 7. For the exciplexes whose emissions could be detected, even a small amount of mixing with the locally excited state of the acceptor (A^*D state) has a measurable effect on k_f that must be taken into account. The details of such an analysis will be provided elsewhere.⁴² A preliminary estimate for V is ca. 600 cm^{-1} .⁴² In view of the uncertainty in this number, the value of 600 cm^{-1} is taken only as a rough guide to the magnitude of V , which is used as a fitting parameter for the electron-transfer data.

H. Determination of ΔG_{-et} . From the fitting of the exciplex spectrum in acetonitrile, the best value of $(\Delta G_{-et})_{cp}$ for the DCA/PMB pair is -2.67 eV. This value is 0.05 eV more negative than that obtained from the redox potentials of this pair ($E^{\text{red}}_A - E^{\text{ox}}_D$, -2.62 eV²⁷). Evidently in this case the increase in free energy of the CRIP due to the loss in solvation compared to the fully solvated radical ions is, within 0.05 eV, offset by the decrease in energy due to the coulombic stabilization. In the case of TCA a similar analysis was not possible due to the weakness of the fluorescence of the exciplexes with this acceptor and to emissions from minor impurities that distorted the spectra. However, by fixing the values of the parameters λ_s , λ_v , and ν_v to those obtained from the DCA spectrum, a value for $(\Delta G_{-et})_{cp}$ of -2.25 eV was obtained for the TCA/durene spectrum by fitting the position of the fluorescence maximum, and the discernible long-wavelength edge of the CT absorption band. This value for $(\Delta G_{-et})_{cp}$ is only 0.03 eV more negative than the redox energy ($E^{\text{red}}_A - E^{\text{ox}}_D$, Table I) of this pair. These small differences are within the experimental error, and so we have simply used the redox energies of the pairs for $(\Delta G_{-et})_{cp}$. We recognize that these free energy values are subject to an error in the absolute scale that is probably ca. 0.1 eV. In addition the relative values are also subject to a smaller error due to different contributions of ground-state stabilization of the CT complexes and also possibly due to different degrees of stabilization of the radical cations as a function of the donor structure, as discussed above. Fortunately, whereas the CT stabilization of the ground-state increases with substitution of the benzene donor, the solvent stabilization effects probably decrease,

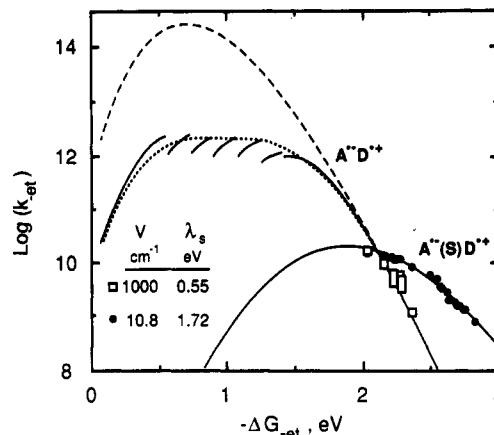


Figure 6. Plots of $\log k_{-et}$ for (circles) solvent-separated radical ion pairs (SSRIP) of TCA and DCA with several alkylbenzene donors (data from Table I and ref 27) and (rectangles) contact radical ion pairs (CRIP) of TCA and the donors shown in Table I, as a function of electron-transfer reaction free energy. The upper and lower limits of the elongated rectangles indicate the rate constants calculated from the two different values of Φ_{solv} obtained by excitation at 410 and 460 nm (Table I). The reactions were carried out in acetonitrile at 25 °C. The curve through the SSRIP data and the dashed curve through the CRIP data are calculated by using eq 5 with $\lambda_v = 0.20$ eV, $\nu_v = 1400$ cm^{-1} , and the other parameters shown in the figure. The solid curve through the CRIP data was calculated by using eq 9 with $\nu_s = 1.4 \times 10^{12}$ s^{-1} . The dotted curve through the CRIP data was calculated by using eq 10, with ν_s^{-1} (7×10^{-13} s) in place of τ_L .

and so these contributions are likely to cancel each other.

I. Fitting of Return Electron-Transfer Data. Shown in Figure 6 are the values of $(k_{-et})_{ss}$ and $(k_{-et})_{cp}$ as functions of the return electron-transfer reaction free energy, ΔG_{-et} .⁴³ For both sets of data the electron-transfer rates decrease as the reaction exothermicity increases (ΔG_{-et} becomes more negative), consistent with a Marcus inverted region effect.¹⁶ The solid curve through the SSRIP ($A^-(S)D^{*+}$) data points and the dashed curve through the CRIP ($A^{*+}D^{*+}$) data points are calculated by using eq 5. For both sets of radical ion pairs, fixed values of 0.20 eV and 1400 cm^{-1} were taken for λ_v and ν_v . For the SSRIP, λ_s and V were variable fitting parameters. For the contact radical ion pairs, a fixed value of 0.55 eV was taken for λ_s , as determined in section G, and only V was a variable parameter. It is important to note that the dependence of k_{-et} on ΔG_{-et} , i.e., the steepness of the curve, is determined solely by ν_v , λ_v , and λ_s . For the $(k_{-et})_{cp}$ data these are not variables, since their values are obtained from the fitting of the CRIP emission spectra. Only the absolute scale of the $(k_{-et})_{cp}$ is affected by V , the adjustable parameter.

The $(k_{-et})_{cp}$ exhibit a much stronger dependence on ΔG_{-et} than the $(k_{-et})_{cp}$ data described by Asahi and Mataga in ref 12b. However, this steep dependence on ΔG_{-et} is almost quantitatively reproduced by using eq 5 with the parameters from the CRIP emission spectra. Further support for this strong ΔG_{-et} dependence comes from the observation that the lifetimes of the exciplex emissions for DCA with durene, PMB and HMB (for which $-\Delta G_{-et} > 2.5$ eV) are all greater than 1 ns and are independent of ΔG_{-et} . As discussed above, this suggests that the $(k_{-et})_{cp}$ for these systems are all significantly less than k_{solv} (6×10^8 s^{-1}), and in fact, values of less than ca. 10^8 s^{-1} are predicted from extrapolation of Figure 6 to exothermicities greater than 2.5 eV. Finally, preliminary estimates for the rates of nonradiative decay of the exciplexes of TCA and DCA with the alkylbenzenes in solvents that are less polar than acetonitrile and in which CRIP lifetimes can be measured directly by using emission spectroscopy indicate a similar steep dependence on ΔG_{-et} in these cases also.²⁴ All of this evidence supports the strong ΔG_{-et} dependence of the $(k_{-et})_{cp}$ data described here.

The solvent reorganization energy required to give a good fit to the SSRIP data, 1.72 eV, is clearly much larger than the value

(42) Mueller, L.; Farid, S.; Gould, I. R.; Young, R. H.; Albrecht, A. C., unpublished results.

(43) The figure contains additional data for $(k_{-et})_{ss}$ taken from ref 27.

of 0.55 eV obtained for the CRIP from the fitting of the exciplex emission spectra. Furthermore, the electronic matrix element V for the solvent-separated radical ion pairs, 10.8 cm^{-1} , is much smaller than that for the contact radical ion pairs, 1000 cm^{-1} .

The errors in the values obtained for the parameters are difficult to estimate. The measured Φ_{ions} are reproducible to within ca. 5% for relative measurements and ca. 10% for absolute measurements.²⁷ As discussed in section C, for several systems different values were obtained for Φ_{solv} for excitation at 410 and 460 nm. Although the reasons for these differences are not known, the main conclusions are the same if the 410-nm data or the 460-nm data are used. The rate constants from both data sets are indicated in Figure 6 as the upper and lower limits of the elongated rectangles. The values of $(k_{\text{et}})_{\text{cp}}$ and $(k_{\text{et}})_{\text{ss}}$ depend upon the values used for k_{solv} and k_{sep} . The k_{solv} values were obtained from direct measurements of the lifetimes of the CRIP by emission spectroscopy and should be fairly accurate. No direct measurements have been made for k_{sep} , and thus an estimated value was used. Errors in k_{sep} have an equal effect on all of the $(k_{\text{et}})_{\text{ss}}$, which means that the errors influence only the value for the fitting parameter V . The resultant error in V is smaller than that in k_{solv} or k_{sep} . For example, an error of 10% or 20% in the value of k_{solv} or k_{sep} would result in an error of 5% or 10% in the corresponding value for V . Due to the steepness of the plot of $\log(k_{\text{et}})_{\text{cp}}$ versus $-\Delta G_{\text{et}}$, the best value for V in this case is also affected, critically, by changes in $-\Delta G_{\text{et}}$. For example, if the $-\Delta G_{\text{et}}$ values are all decreased by 50 mV, then the best value of V decreases by ca. 250 cm^{-1} . Taking all of these admittedly semiquantitative considerations into account, we estimate that V for the CRIP probably lies between 700 and 1300 cm^{-1} . The low end of this range for V is consistent with the preliminary estimate of this parameter obtained from radiative rate constant data⁴² (see section G).

J. Nonperturbative Treatments. Our working formula, eq 5, results from first-order time-dependent perturbation theory^{33,39a} and holds only for small V . For the SSRIP, V is indeed small (see further below). For the CRIP, however, V is large enough (e.g., $V \gg k_B T$) that we must consider whether eq 5 is applicable in this case. We discuss below two nonperturbative theories that should extend to rather large values of V . These theories corroborate eq 5 when $F_j^{1/2}V$ is small (even if V itself is large) for certain of the Franck-Condon factors F_j . These criteria are actually met for the CRIP over the experimental range of ΔG_{et} . For extrapolation to smaller exothermicities, however, a nonperturbative theory is more appropriate.

Electron-transfer rates are often described in terms of adiabaticity and nonadiabaticity, and the validity of eq 5 is often identified with nonadiabaticity.^{33d-f,44} Indeed, in the conventional (avoided) level-crossing picture,⁴⁴ most passages through the crossing region follow the nonadiabatic (diabatic) path if V is small and the adiabatic path if V is large. (This observation should not be confused with another, that the adiabatic path leads to electron transfer in the Marcus normal region, but a combination of adiabatic and nonadiabatic paths is required for electron transfer in the inverted region.^{33f,44}) Nevertheless, the actual issue is the validity of perturbation theory.

A standard nonperturbative treatment by semiclassical transition-state theory results in eq 8.^{33f,44,45} In this case λ is the total

$$k_{\text{et}} = \nu_n \kappa_{\text{el}} \exp \left[-\frac{(\Delta G_{\text{et}} + \lambda)^2}{4\lambda k_B T} \right] \quad (8a)$$

$$\lambda = \lambda_v + \lambda_s \quad (8b)$$

$$\nu_n^2 = \frac{\nu_v^2 \lambda_v + \nu_s^2 \lambda_s}{\lambda_v + \lambda_s} \quad (8c)$$

reorganization energy (eq 8b), ν_s is a characteristic frequency for

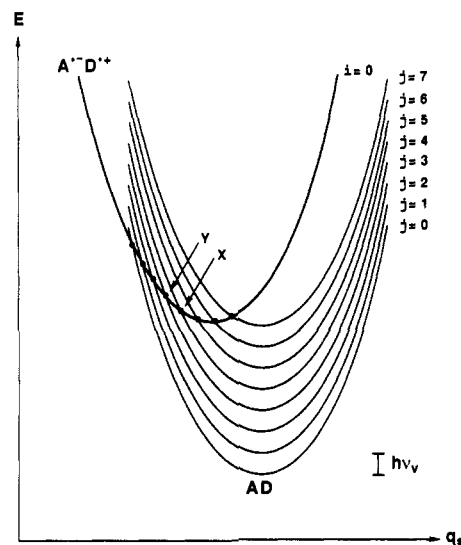


Figure 7. Energy of the initial vibronic state ($A^{\cdot-}D^{+\cdot}$, $i=0$) and several final vibronic states (AD , various j) versus a representative low-frequency (e.g., solvent) nuclear coordinate (q_s). Successive final-state curves are displaced vertically by a high-frequency vibrational quantum ($h\nu_v$). Each level-crossing (e.g., point X or Y) gives rise to a separate vibronic electron transfer process (a $0 \rightarrow j$ nonradiative transition) whose rate is calculated by a Landau-Zener formula with a vibronic matrix element of magnitude $F_j^{1/2}V$. For large j , this quantity is small and the golden rule result (the j th term in eq 5) is regained. For small j , the golden rule is invalid.

motion of the solvent, and ν_n is a weighted average of the high and low vibrational frequencies ν_v and ν_s . The "electronic transition probability", κ_{el} , is the probability (≤ 1) that a transition from the ion pair electronic state to the neutral state occurs when a level crossing is encountered. Equation 8 can be used to obtain a fit (not shown) to the CRIP data in Figure 6, with 1.4 eV for λ and $4.4 \times 10^{11} \text{ s}^{-1}$ for $\nu_n \kappa_{\text{el}}$. This value for λ , however, is almost twice that obtained from fitting the CT emission spectrum, 0.75 eV. Alternatively, using 0.75 eV for λ in eq 8 gives a curve with a slope (on the semilogarithmic plot of Figure 6) more than 3 times that of the actual data in the experimental range and requires an unrealistically large value, $4 \times 10^{22} \text{ s}^{-1}$, for $\nu_n \kappa_{\text{el}}$. Regardless of whether eq 5 is valid, eq 8 clearly does not fit the data.

The derivation of eq 8 by transition-state theory incorporates an assumption that the high-frequency mode ($h\nu_v \gg k_B T$) can be treated by classical statistical mechanics just as low-frequency modes ($h\nu_s \ll k_B T$) are conventionally treated.^{44,45} In contrast, although the derivation of eq 5 introduces both kinds of mode on the same quantum-mechanical basis, approximations that are valid for the low-frequency modes allow their influences to be incorporated in a classical activation factor (the terms following V^2 in eq 5), whereas the high-frequency mode makes discrete contributions of a quite different form.^{33c,e} This result suggests that in a semiclassical transition-state theory, only the low-frequency modes should be treated by classical statistical mechanics. The high-frequency modes can be treated quantum mechanically by use of vibronic initial and final states $\Psi_{A-D^+} \chi_{A-D^+,i}$ and $\Psi_{AD} \chi_{AD,j}$ rather than purely electronic states Ψ_{A-D^+} and Ψ_{AD} . Here $\chi_{A-D^+,i}$ and $\chi_{AD,j}$ are the i th and j th states of the ν mode appropriate to the ionic and neutral species. Because of the large energy required to populate vibrationally excited initial states, only $i=0$ needs to be considered, but various numbers of quanta (j) are possible in the final state.

For an appropriate refinement of eq 8, we are thus led to the picture in Figure 7, in which each parabola represents the energy of a vibronic state as a function of some solvent coordinate (q_s) and governs the motion of the solvent for that vibronic state. Whenever a level crossing is encountered, there is a certain probability (transmission probability, κ_j) that the system jumps from the initial, ionic state ($i=0$) to a final, neutral state (the j th). That probability is evaluated by adaptation of the Landau-Zener theory⁴⁶ in refs 44 and 45. We further assume that

(44) Newton, M.; Sutin, N. *Annu. Rev. Phys. Chem.* 1984, 35, 437.

(45) Brunschweig, B. S.; Logan, J.; Newton, M. D.; Sutin, N. *S. J. Am. Chem. Soc.* 1980, 102, 5798.

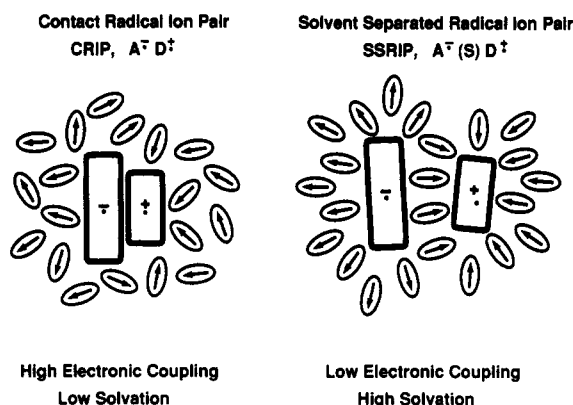


Figure 8. Schematic representation of a contact and a solvent-separated radical ion pair in a polar solvent. The ovals represent the acetonitrile solvent with dipole moments indicated by the arrows.

the solvent coordinates and momenta initially have a Boltzmann distribution in energy. Each vibronic transition acquires an activation factor as in eq 5. The sum of the individual vibronic transition rates is the net electron-transfer rate, eq 9.

$$k_{-et} = \sum_{j=0}^{\infty} \nu_j \kappa_j \exp \left[-\frac{(j h \nu_v + \Delta G_{-et} + \lambda_s)^2}{4 \lambda_s k_B T} \right] \quad (9a)$$

$$\kappa_j = 2P_j(1 + P_j)^{-1} \quad \text{for } j h \nu_v + \Delta G_{-et} + \lambda_s > 0 \quad (9b)$$

$$\kappa_j = 2P_j(1 - P_j) \quad \text{for } j h \nu_v + \Delta G_{-et} + \lambda_s < 0 \quad (9c)$$

$$P_j = 1 - \exp \left[-\frac{F_j V^2}{2 \nu_s} \left(\frac{4 \pi^3}{h^2 \lambda_s k_B T} \right)^{1/2} \right] \quad (9d)$$

The quantity $F_j^{1/2} V$ in eq 9d is the magnitude of the matrix element coupling vibronic states, with V still representing the corresponding purely electronic matrix element. The exothermicity of the j th vibronic transition is $-(j h \nu_v + \Delta G_{-et})$. Note that eq 9 reduces to eq 5, term by term, when V is small or ν_s is large, whereas eq 8 does not. The criterion for this reduction is that the quantities $F_j^{1/2} V$ be small, rather than V itself.

The extra parameter required by eq 9, ν_s , can be estimated from solvent dynamical effects on electron-transfer rates. With use of a continuum model of solvation response, the reciprocal of the "longitudinal" relaxation time, $\tau_L = 0.2$ ps, might be taken for ν_s .⁴⁷ Experimental solvation times from dynamical Stokes shift measurements in acetonitrile, however, are consistently longer; values between 0.4 and 0.9 ps are reported.⁴⁷ Furthermore, the lifetime for intramolecular electron transfer in bianthryl in acetonitrile, which is suggested to be solvation controlled, has been measured to be 0.7 ps.^{47b,c} The reciprocal of this lifetime, $1.4 \times 10^{12} \text{ s}^{-1}$, thus probably represents a reasonable estimate for ν_s .

Equation 9 is plotted in Figure 6 (solid curve) by using this value for ν_s , and the same values for the CRIP parameters as were used with eq 5. The two curves agree well throughout the experimental range of ΔG_{-et} , confirming the perturbation treatment over this range, and thus the use of eq 5 to estimate V for the CRIP. At smaller exothermicities, the curves diverge and eq 5 appears to give an unrealistically high maximum rate, whereas eq 9 behaves more reasonably. (In contrast, for the SSRIP, V is small enough that eqs 5 and 9 agree within 0.4% throughout the ΔG_{-et} range of Figure 6.) The periodic discontinuities near

the maximum of eq 9 are typical of a Landau-Zener theory. These and further aspects of eq 9 are discussed in the Appendix. Additional calculations show that the maximum rate from eq 9 is approximately proportional to the "solvent frequency" ν_s , and hence is governed by solvent dynamics. Rather than trying to refine eq 9, we turn to a more sophisticated nonperturbative treatment of electron-transfer and solvation dynamics.

Jortner and Bixon⁴⁸ treat the high-frequency mode quantum mechanically, and they assume that the solvent relaxation has a Debye frequency spectrum. Their result in our notation is given in eq 10. Equation 10 is like eq 5 except for the factor $(1 + H_j)^{-1}$,

$$k_{-et} = \sum_{j=0}^{\infty} F_j V^2 \left(\frac{4 \pi^3}{h^2 \lambda_s k_B T} \right)^{1/2} \times (1 + H_j)^{-1} \exp \left[-\frac{(j h \nu_v + \Delta G_{-et} + \lambda_s)^2}{4 \lambda_s k_B T} \right] \quad (10a)$$

$$H_j = \frac{8 \pi^2 F_j V^2 \tau_L}{h \lambda_s} \quad (10b)$$

which keeps the summand from becoming too large when V is large. Equation 10 again reduces to eq 5 if V or τ_L is small. (For further discussion see ref 48.) Equation 10 is plotted in Figure 6 as the dotted line through the CRIP data. As discussed earlier, experimental solvation times in acetonitrile are somewhat longer than the Debye longitudinal relaxation time τ_L , so we have arbitrarily replaced τ_L by our empirical value of ν_s^{-1} . Equation 10 agrees quantitatively with the perturbation theory that was used to fit the CRIP data, eq 5, throughout the experimental range of ΔG_{-et} , providing further support for that treatment. It agrees semiquantitatively with eq 9 near their maxima but lacks the oscillation and discontinuities of the Landau-Zener treatment. If we had not replaced τ_L by ν_s^{-1} , the agreement with the perturbation theory would have been even better, and the maximum rate would have been ca. 3.4 times higher than that shown in Figure 6. Equations 9 and 10 are compared further in the Appendix. For the SSRIP, eqs 5 and 10 agree within 0.5% throughout the ΔG_{-et} range of Figure 6.

K. Structure of the Contact and Solvent-Separated Radical Ion Pairs. The large differences in electronic coupling and solvent reorganization for the two sets of ion pairs can easily be understood on the basis of the simple pictorial representation of these two species shown in Figure 8, in which the solvent molecules are represented by the ovals, with the dipole moments as indicated. It is well-known that the solvent reorganization depends upon the center-to-center distance of the ionic centers in an ion pair.¹⁶ There are two major differences in the state of solvation of the contact and solvent-separated radical ion pairs. First, there are no solvent molecules between the ions in the CRIP. Second, because the ions in the CRIP are close together, there is considerable cancellation of their orienting influence on the outer solvent shells and, to a lesser extent, on the inner shell. Both effects reduce the overall solvation of the ions in the CRIP compared to the SSRIP. In the final, nonionic state, there should be comparatively little solvation of the contact and solvent-separated neutral molecules. Hence λ_s , which represents the change in solvation between ionic and neutral states, should be considerably larger for the SSRIP than for the CRIP, as observed.

According to simple dielectric continuum models, the solvent reorganization energies of otherwise equivalent electron transfer and self-exchange reactions should be the same.^{16a,33f,44} As discussed in a previous publication, however,²⁷ the solvent reorganization energy, λ_s , of ca. 1.7 eV for the SSRIP reactions is much larger than the reorganization energies that have been measured for self-exchange reactions for organic radical ions in acetonitrile (ca. 0.25–0.5 eV),⁴⁹ which must also include some skeletal re-

(46) For discussions of Landau-Zener theory, including criticisms and generalizations, see: (a) Baede, A. P. M. *Adv. Chem. Phys.* **1975**, *30*, 463. (b) Nikitin, E. E. In *Chemische Elementarprozesse*; Hartmann, H., Ed.; Springer: New York, 1968. (c) Kuznetsov, A. M.; Ulstrup, J.; Vorotyntsev, M. A. In *The Chemical Physics of Solvation*; Dogonadze, R. R.; Kálman, E.; Kornyshev, A. A.; Ulstrup, J., Eds.; Elsevier: New York, 1988; part C. (47) (a) Maroncelli, M.; MacInnis, J.; Fleming, G. R. *Science* **1989**, *243*, 1674. (b) Kahlow, M. A.; Kang, T. J.; Barbara, P. F. *J. Phys. Chem.* **1987**, *91*, 6452. (c) Kahlow, M. A.; Kang, T. J.; Barbara, P. F. *J. Chem. Phys.* **1988**, *88*, 2372.

(48) (a) Jortner, J.; Bixon, M. *J. Chem. Phys.* **1988**, *88*, 167. (b) Rips, I.; Jortner, J. *J. Chem. Phys.* **1987**, *87*, 2090.

(49) Ebersson, L. In *Advances in Physical Organic Chemistry*; Gold, V., Bethell, D., Eds.; Academic Press: London, 1982; Vol. 18, p 79.

organization (i.e., a contribution from λ_s). However, the solvent reorganization energy for the CRIP reactions ($\lambda_s = 0.55$ eV) is much closer to these values, which supports a model in which the self-exchange reactions occur in contact and not in a solvent-separated configuration. The reason for this is readily apparent by inspection of Figure 6. It is clear that for the special case of a self-exchange reaction ($\Delta G_{et} = 0$), electron transfer is much faster if the donor and acceptor are in contact. Electron transfer within a solvent-separated radical ion pair is very slow when the reaction is thermoneutral both because of the small electronic coupling and because of the large reorganization energy. In contrast, for an electron-transfer reaction that is very exothermic, say by more than 2 eV, reaction in the solvent-separated pairs can actually be faster than in the contact pairs, despite the unfavorable matrix element, because the large exothermicity can be accommodated by the large reorganization energy. In the contact pairs, very exothermic reactions will be very slow despite the large electronic coupling, because the small reorganization energy cannot accept the large reaction exothermicity. Thus, for reactions in acetonitrile in which solvation from the CRIP to SSRIP can readily occur, return electron-transfer reactions are more likely to occur in the solvent-separated configuration if the reactions are highly exothermic and thus will be characterized by large reorganization energies, as observed in many ion pair systems.^{12a,14,15}

The electronic coupling matrix element, V , is understandably much larger in the contact pairs than in the solvent-separated pairs. V is usually assumed to depend exponentially upon the distance between the donor and acceptor, eq 11.^{33,44} The rate of atten-

$$V_2 = V_1 \exp(-\beta(r_2 - r_1)/2) \quad (11)$$

uation of V with distance is determined by the magnitude of the factor β , which will depend upon the system. Reasonable estimates for the center-to-center distances in contact and solvent-separated radical ion pairs are ca. 3.5 and ca. 6–8 Å, respectively.¹ Using these values for r_1 and r_2 and using 1000 and 10.8 cm⁻¹ for V_1 and V_2 , we obtain a value for β of 2.3 ± 0.3 Å⁻¹. Literature values for β typically range from 1 to 2 Å⁻¹.⁴⁴ The value obtained here is obviously rather high, although the smaller values of β are usually found for systems in which there is through-bond coupling between the donor and acceptor, which is clearly not the case in the ion pairs. The value of β obtained here should be considered to be only a rough estimate since the exponential distance dependence of V is probably valid only for large center-to-center distances where only the overlap of the tails of the wave functions need be considered. When the donor and acceptor are in contact, the detailed nodal structure of the wave functions becomes important⁵⁰ and eq 11 becomes semiquantitative at best.

It is now clear both from the data shown in Figure 6 and from the picosecond transient absorption experiments^{11,12,20,21} that return electron transfer within the contact radical ion pairs can be extremely rapid. We now also understand that this is due to the extremely large electronic coupling in these ion pairs, which means that for systems in which the thermal and Franck-Condon factors are optimal, very high return electron-transfer rates are expected. If the present system is representative, $(k_{-et})_{cp}$ typically exceeds 10^{10} s⁻¹ throughout a ΔG_{et} range of 0 to -2 eV. In this range, other processes such as emission, intersystem crossing, or chemical reaction cannot compete very efficiently with return electron transfer. The donor and acceptor redox potentials that are required for efficient ground-state CT complex formation typically result in ΔG_{et} values in this range. Therefore it is not surprising that emission or chemical reaction is rarely reported for excited CT complexes in polar media. The rate of return electron transfer does, however, decrease rapidly with increasing exothermicity, so that in the present case, for return electron transfer exothermicities larger than 2.4 eV, the rate of return electron transfer falls below ca. 5×10^8 s⁻¹. Consistent with the rapid decrease in $(k_{-et})_{cp}$ is the observation that for the CRIP of DCA with the

alkylbenzenes ($-\Delta G_{et} > 2.5$ eV) the $(k_{-et})_{cp}$ must be small compared to the rate of solvation, k_{solv} , since the emission lifetimes of these CRIP do not depend upon ΔG_{et} , as discussed earlier.

In the previous study by Asahi and Mataga,^{12b} the rates of return electron transfer were measured for contact radical ion pairs of pyromellitic dianhydride with (among others) several alkylbenzenes as donors. The rates in those systems are in general higher than those obtained here using the cyanoanthracene acceptors, and a smaller dependence of $(k_{-et})_{cp}$ on ΔG_{et} was observed.^{12b} However, we have observed previously that the rates of electron transfer in ion pair systems can be sensitive to small changes in molecular geometry.^{14b,27} Indeed, smaller molecular dimensions appear to be correlated with larger electronic coupling matrix elements, which might account for the higher rates with the pyromellitic dianhydride acceptors compared to the cyanoanthracenes. Furthermore, the reorganization energies are not expected to be the same for both types of acceptor. The differences in electron-transfer rate can be understood if the reorganization energies for the pyromellitic dianhydride systems are larger than those for the cyanoanthracenes, especially if the reorganization energy is not constant in the pyromellitic dianhydride systems.⁵¹ The results of the study by Asahi and Mataga together with those of the present work are consistent with the suggestion that rates of electron transfer are a sensitive function of molecular structure.^{14b,27}

It is interesting that the rates of return electron transfer obtained here for the CRIP and the SSRIP are all in the Marcus inverted region. With the present donor/acceptor pairs, it is not possible to observe the "normal" region because the accessible range of redox potentials results in ion pair energies that are always larger than the total reorganization energy. Indeed, the present results suggest that the normal region for return electron transfer in any contact pair system would be difficult to study since the ion pair energy would have to be less than ca. 0.8 eV, in which case mixing of the neutral ground and ion pair states might become important. Clearly the best possibility of observing both the normal and inverted regions is in the solvent-separated pairs, which have larger total reorganization energies, and indeed such behavior has been observed in several solvent-separated ion pair systems.^{12,15}

Conclusion

A series of donors has been studied for which excitation of free and complexed TCA leads to different quantum yields for free-radical ion formation. This is consistent with the formation of CRIP upon excitation of the complexes and the formation of SSRIP upon quenching of the free acceptor in solution. The quantum yield data together with the CRIP emission lifetimes allow the determination of the rates of return electron transfer and solvation for the CRIP. The rates of solvation are found to vary with the structure of the donor, perhaps as a result of differing degrees of solvation of the donor radical cations in the CRIP and SSRIP. Consistent with a simple picture of these species, the return electron transfer within the CRIP, compared to the SSRIP, is characterized by a much larger (ca. 2 of orders of magnitude) electronic coupling matrix element and a much smaller (by ca. 1 eV) low-frequency (solvent) reorganization energy. A comparison of perturbative and nonperturbative treatments of the return electron data for the CRIP supports the use of the perturbation treatment for electron-transfer reactions that are deep

(50) (a) Friedman, H. L.; Newton, M. D. *Faraday Discuss. Chem. Soc.* **1982**, *74*, 73. (b) Newton, M. D. *Int. J. Quant. Chem. Symp.* **1980**, *14*, 363.

(51) Indeed, from preliminary studies of the emission spectra of the alkylbenzene/pyromellitic dianhydride systems in carbon tetrachloride we have obtained experimental evidence that the reorganization energies in these cases are significantly larger than those for the cyanoanthracene acceptor systems in the same solvents. In addition, whereas the emission spectra of the cyanoanthracene systems suggest that their reorganization energies do not depend upon the alkylbenzene donor, the spectra of the pyromellitic dianhydride systems indicate that their reorganization energies are not constant. In addition, the picosecond transient absorption experiments described in ref 12b can be complicated by absorptions due to the SSRIP, as discussed in footnote 52 for the case of the TCA pairs. After these observations are taken into account, the data in ref 12b might be understood in terms of the electron-transfer theories described here. The results of the emission studies will be published elsewhere.

TABLE III: Comparison of Calculations According to Eqs 5 and 9 Using the Parameters Applied To Fit the CRIP Data^a

<i>j</i>	$F_j^{1/2}V^b$	$\kappa_j^{b,c}$			% contribution ^d to k_{-et}		
		inverted	normal	perturbation	$-\Delta G_{-et} = 1.5$	$-\Delta G_{-et} = 2.0$	$-\Delta G_{-et} = 2.5$
0	562	<10 ⁻⁴	1.00	79			
1	603	<10 ⁻⁴	1.00	91			
2	458	<10 ⁻⁴	1.00	52			
3	284	<10 ⁻⁴	1.00	20			
4	152	0.11	0.97	5.8	5		
5	73	0.5	0.65	1.3	65	4	
6	32	0.21	0.21	0.25	27	33	
7	13	0.041	0.041	0.042	2	45	2
8	4.9		6.0×10^{-3}			17	17
9	1.7		7.7×10^{-4}			2	42
10	0.6		9.0×10^{-5}				31
11	0.19		9.3×10^{-6}				7
12	0.06		9.0×10^{-7}				
$(k_{et})_{eq9}/(k_{et})_{eq5}^e = 0.16$						0.87	0.998

^a $V = 1000 \text{ cm}^{-1}$, $\lambda_v = 0.20 \text{ eV}$, $\lambda_s = 0.55 \text{ eV}$, $\nu_s = 1400 \text{ cm}^{-1}$; solvent frequency (ν_s) = $1.4 \times 10^{12} \text{ s}^{-1}$. ^b A nonradiative $0 \rightarrow j$ transition has a matrix element $F_j^{1/2}V$ and a transmission coefficient κ_j . ^c Values of κ_j as evaluated by eqs 9b,c and the perturbation limit of both (ν_s^{-1} times the preexponential factor in eq 5a). The first two calculations apply if the $0 \rightarrow j$ vibronic transition is in the Marcus inverted or normal region, ($j h \nu_s + \Delta G_{-et} + \lambda_s$) negative or positive, respectively; the third applies in either region if $F_j^{1/2}V$ is small enough. For $j \geq 8$ all three values agree to the number of figures shown. ^d Contributions to k_{-et} from the different $0 \rightarrow j$ transitions, calculated for three arbitrary values of $-\Delta G_{-et}$ (in electronvolts). Entries above (below) the horizontal bars are in the inverted (normal) region. ^e Ratio of the rate constants evaluated by eqs 9 and 5 for the different values of $-\Delta G_{-et}$.

in the inverted region, even when the matrix elements are as large as 1000 cm^{-1} . The data in Figure 6 show that the return electron transfer within the CRIP could be either much faster (at small exothermicities) or much slower (at large exothermicities) than the corresponding rate in the SSRIP for these TCA systems. Thus in the latter case the dominant reaction of the CRIP ultimately becomes solvation to form the SSRIP. In the other extreme the energy-wasting return electron transfer, which can have a rate that exceeds 10^{12} s^{-1} , becomes the dominant reaction of the CRIP. The wide range in rates for this energy-wasting step could account for the wide variation in observations related to emission and chemistry from excitation of CT complexes.⁵²

Experimental Section

Materials. Acetonitrile (Baker, HPLC grade) was used as received. 9,10-Dicyanoanthracene (DCA) (Kodak) was purified by crystallization from pyridine and acetonitrile. 2,6,9,10-Tetracyanoanthracene (TCA) was prepared as described earlier⁵³ and was purified by repeated chromatography on silica gel eluting with methylene chloride. 1,2,4-Trimethylbenzene (Kodak) was purified by distillation. Durene (Aldrich), pentamethylbenzene (Aldrich), and hexamethylbenzene (Aldrich) were purified by repeated crystallization from ethanol. 4-Methoxystilbene (Kodak) and 4,4'-dimethoxystilbene (Aldrich) were recrystallized twice from acetonitrile. 1,2,3,4-Tetramethylbenzene (API Standard Reference Materials) and 1,2,3,5-tetramethylbenzene (API Standard Reference Materials) were used as received.

Steady-State Spectroscopy. Steady-state emission spectra were recorded by using a Spex Fluorolog 212 spectrometer. Absorption spectra were recorded by using a Perkin-Elmer Lambda-9 spectrometer, equipped with a 7000 series datastation. Solutions were analyzed in 1-cm² quartz cuvettes equipped with arms for freeze-pump-thaw degassing or for argon purging. In all the

experiments, oxygen was removed by using one of these two methods.

Time-Resolved Spectroscopy. A conventional transient absorption apparatus was used that consisted of a Questek 2000 excimer laser (308 nm, ca. 15 ns, 100 mJ) which pumped a Lumonics EPD-330 dye laser. DPS (410 nm, ca. 1 mJ), bis-MSB (427 nm, ca. 1 mJ), and coumarin-460 (460 nm, ca. 2 mJ) were used to excite the acceptors and other compounds. A pulsed (PRA M-305) Osram XBO-150W1 xenon arc lamp (Oriel 66060 housing, PRA 302 power supply) was used as the monitoring light source. The monitoring light was passed through an ISA H-20 monochromator and was detected by using six dynodes of an RCA 4840 photomultiplier tube (PMT). The output from the PMT was monitored by using a Nicolet 4094A digital oscilloscope with a Model 4175 plug-in. The quantum yields for free-radical ion formation from the SSRIP ($(\Phi_{\text{ions}})_{ss}$) were reported previously.²⁷ Quantum yields for excitation at 460 nm were measured relative to those determined previously for excitation at 410 nm. In our preliminary work¹⁷ we used the triplet state of phenanthrene quinone, observed at 485 nm, as a relative actinometer for these two excitation wavelengths. However, we recently discovered that the relative ion yields obtained in this way were somewhat irreproducible and different from those obtained by using other actinometer reactions. The yield data given here are obtained by using new relative actinometers which are based on electron-transfer reactions, using sensitizers that absorb similarly at 410 and 460 nm. With 4-methoxystilbene as a radical cation monitor, the yields of free-radical cations were measured for quenching of the excited singlet state of 10-chloro-*N*-methylacridinium perchlorate in acetonitrile with the electron donors hexaethylbenzene and 1,2,4,5-tetraisopropylbenzene and also for quenching of the excited singlet state of 2,6-bis[*p*-ethylphenyl]-4-[*p*-cyano-phenyl]pyrylium perchlorate with the same donors and also with biphenyl. With these five actinometers, consistent results (within 5%) were obtained for the relative yields for the TCA systems at the two excitation wavelengths.

Fluorescence lifetime measurements were performed using the technique of single-photon counting, using an apparatus which will be described in detail elsewhere.²⁴

Acknowledgment. We thank Professor F. C. DeSchryver (Leuven, Belgium) for providing the single-photon-counting lifetime deconvolution software.

Appendix. Comments on the Nonperturbative Theories

The periodic discontinuities near the maximum of eq 9 (see Figure 6) mark the points at which, for various j values, ($j h \nu_s +$

(52) (a) After submission of this work, Mataga et al. reported the results of picosecond transient absorption studies on the TCA/alkylbenzene systems in acetonitrile.^{52b} In that work the data were interpreted to indicate a much weaker dependence of $(k_{-et})_{ss}$ on ΔG_{-et} than that described in the present work. The data described in ref 52b, however, could be complicated by absorptions due to the SSRIP that would be indistinguishable from the CRIP in those experiments. Indeed, a preliminary evaluation suggests that with our experimental values for τ_{CRIP} , Φ_{soln} , and $(\Phi_{\text{ions}})_{ss}$, reasonable fits to all of the decay profiles in ref 52b can be obtained from the sum of the calculated decays of both the CRIP and the SSRIP, using k_{sep} of $7 \times 10^8 \text{ s}^{-1}$ as the only variable. Interestingly, such experiments may provide the best method for determining this rate constant. If k_{sep} is indeed $7 \times 10^8 \text{ s}^{-1}$ instead of our estimate of $5 \times 10^8 \text{ s}^{-1}$, the matrix element, V , for the SSRIP should be increased by ca. 20%. (b) Asahi, T.; Mataga, N.; Takahashi, Y.; Miyashi, T. *Chem. Phys. Lett.* **1990**, *171*, 309.

(53) Mattes, S. L.; Farid, S. J. *Am. Chem. Soc.* **1982**, *104*, 1454.

$\Delta G_{-et} + \lambda_s$) passes through zero, the situation changes from Marcus inverted to normal-region behavior, and the expression for κ_j , eqs 9b,c, changes discontinuously. Upon inspection of eqs 9 it is clear that these discontinuities are severe only when V is large or ν_s is small. They may be an artifact of the assumption that just one solvent coordinate enters the Landau–Zener formalism (see ref 46b, section 8). The absolute rates near the maximum may also be diminished somewhat by the fact that the probability of reaching a higher crossing point (e.g., point Y in Figure 7) is affected by the probability of passing by lower crossing points (e.g., point X in Figure 7) without abandoning the initial state curve.⁵⁴ An estimate of the individual contributions to the total rate indicates that this correction is probably rather small, perhaps <30%, and is confined largely to the region near the maximum rate. These considerations concern the behavior of eq 9 near the maximum, where solvent dynamical effects dominate the rate and a more detailed treatment of solvent dynamics is eventually required. Hence we have made no attempt to improve upon eq 9 in this region.

The relationship between eq 5 and eq 9 and their eventual divergence at small exothermicities can be understood easily with the aid of Table III. The magnitude of the matrix element governing the $0 \rightarrow j$ nonradiative transition (i.e., the return

electron-transfer process that leaves j quanta in the v mode of the final state) is $F_j^{1/2}V$. This quantity is large, e.g., compared to $k_B T$, for $j = 0-3$ but decreases rapidly for larger j . Consequently, perturbation theory should fail for small j but be accurate for large j . In fact, the transmission coefficients κ_j are poorly approximated by perturbation theory for $j = 0$ to ca. 5 but well approximated for $j > 6$, irrespective of the size of ΔG_{-et} . However, the weight given to each κ_j by the thermal exponential is dependent upon the size of ΔG_{-et} . This weight is greatest for a particular j when $(j h \nu_s + \Delta G_{-et} + \lambda_s)$ is closest to zero (see horizontal bars, columns 6–8, Table III), and it is approximately these j values that dominate the overall rate. The overall rate is well approximated by perturbation theory when these dominant j values are large (e.g., $-\Delta G_{-et} > 2.0$ eV) are poorly approximated otherwise (bottom line, Table III).

The agreement between eqs 9 and 10 deteriorates, not surprisingly, if different characteristic times are used, i.e., if τ_L is not replaced by ν_s^{-1} . The agreement found with this replacement (see Figure 6) itself seems to result from a numerical coincidence. The j th preexponential factor in eq 10 has a maximum value shown in eq 12, whereas $\nu_s \kappa_j$ in eq 9 has a maximum value of ν_s . Nev-

$$\left(\frac{\lambda_s}{16\pi k_B T} \right)^{1/2} \tau_L^{-1} \approx 0.65 \tau_L^{-1} \quad (12)$$

ertheless, since λ_s could typically be in the range 0.1–0.7 eV for the contact pairs, and it appears in eq 12 as the square root, the maximum values of the summands in eqs 9 and 10 will rarely differ by a large factor. For small values of V or of τ_L and ν_s^{-1} , eqs 9 and 10 agree because both reduce to eq 5.

(54) (a) Maier, W. B., II *J. Chem. Phys.* **1974**, *60*, 3588. For further discussion of the multistate Landau–Zener problem see: (b) ref 43b, Section 7; ref 43c, Section 4.4.1. (c) Demkov, Y. N.; Osherov, V. I. *Zh. Eksp. Teor. Fiz.* **1968**, *53*, 1589 [*Sov. Phys. JETP* **1968**, *26*, 916]. (d) Vorotyntsev, M. A.; Dogonadze, R. R.; Kuznetsov, A. M. *Fiz. Tverd. Tela* **1970**, *12*, 1605 [*Soviet Phys., Solid State* **1970**, *12*, 1273].

Supramolecular Photochemistry and Photophysics. Mutual Inhibition of Host and Guest Photochemistry and Luminescence in the Adduct of an Anthraceno–Crown Ether with $\text{Pt}(\text{bpy})(\text{NH}_3)_2^{2+}$

Luca Prodi,^{1a} Roberto Ballardini,^{*1b} Maria Teresa Gandolfi,^{*1a} Vincenzo Balzani,^{1a} Jean Pierre Desvergne,^{1c} and Henri Bouas-Laurent^{1c}

Dipartimento di Chimica "G.Ciamician" dell' Università, Bologna, Italy, Istituto FRAE-CNR, Bologna, Italy, and Laboratoire de Photophysique et Photochimie Moléculaire, CNRS URA 348, Université de Bordeaux I, Talence 33405 Cedex, France (Received: April 25, 1990; In Final Form: September 25, 1990)

$\text{Pt}(\text{bpy})(\text{NH}_3)_2^{2+}$ forms a 1:1 adduct with the anthraceno–crown ether **2**. The adduct formation causes (i) strong changes in the absorption spectra of the two components, (ii) the quenching of the luminescence and photoreactivity of both $\text{Pt}(\text{bpy})(\text{NH}_3)_2^{2+}$ and **2**, and (iii) the appearance of a new, broad, low-energy emission band at 77 K. It is suggested that the adduct exhibits a sandwich-type conformation in which the Pt complex is inserted between the two aromatic moieties of **2**. Such a structure allows the stabilization of the adduct via both hydrogen bonds and π – π interactions and accounts for the mutual protection of the two components toward their luminescence and photoreactivity.

Introduction

In the past few years, there has been an increasing interest in the photochemistry and photophysics of supramolecular species² and, in particular, of host–guest systems.^{3–8} Perturbation induced

by a host can offer a means to control in a selective way the excited-state behavior of a guest and vice versa. We report here a system where the formation of a host–guest adduct controls the photochemical and photophysical behavior of both host and guest species.

The $\text{Pt}(\text{bpy})(\text{NH}_3)_2^{2+}$ (bpy = 2,2'-bipyridine) complex ion (**1**, Chart 1) is known to form adducts with crown ethers⁹ because its ammonia ligands give rise to hydrogen bonds with the oxygen atoms of the crown ring. Furthermore, $\text{Pt}(\text{bpy})(\text{NH}_3)_2^{2+}$ is flat, and thus it can be sandwiched by aromatic crown ethers of suitable structure to give rise to host–guest type adducts.^{5,9} In such cases,

(1) (a) Dipartimento di Chimica "G.Ciamician" dell' Università, Bologna, Italy. (b) Istituto FRAE-CNR, Bologna, Italy. (c) Laboratoire de Photophysique et Photochimie Moléculaire, CNRS URA 348, Université de Bordeaux I, Talence 33405 Cedex, France.

(2) Balzani, V., Ed. *Supramolecular Photochemistry*; Reidel: Dordrecht, Holland, 1987.

(3) Lehn, J.-M. *Angew. Chem., Int. Ed. Engl.* **1988**, *27*, 89.

(4) Ramamurthy, V.; Eaton, D. F. *Acc. Chem. Res.* **1988**, *21*, 300.

(5) (a) Ballardini, R.; Gandolfi, M. T.; Balzani, V.; Kohnke, F. H.; Stoddart, J. F. *Angew. Chem., Int. Ed. Engl.* **1988**, *27*, 692. (b) Ballardini, R.; Gandolfi, M. T.; Prodi, L.; Ciano, M.; Balzani, V.; Kohnke, F. H.; Shahriri-Zavareh, H.; Spencer, N.; Stoddart, J. F. *J. Am. Chem. Soc.* **1989**, *111*, 7072. (c) Gandolfi, M. T.; Zappi, T.; Ballardini, R.; Prodi, L.; Balzani, V.; Stoddart, J. F.; Mathias, J. P.; Spencer, N. *Gazz. Chim. Ital.*, in press.

(6) Lohr, H. G.; Vogtle, F. *Acc. Chem. Res.* **1985**, *18*, 65.

(7) Diederich, F. *Angew. Chem., Int. Ed. Engl.* **1988**, *27*, 362.

(8) Shinkai, S.; Manabe, O. *Top. Curr. Chem.* **1984**, *121*, 67.

(9) Colquhoun, H. M.; Stoddart, J. F.; Williams, D. J. *Angew. Chem., Int. Ed. Engl.* **1986**, *25*, 487.